NOTICE

The quality of this microform is heavily dependent upon the quality of the original thesis submitted for microfilming. Every effort has been made to ensure the highest quality of reproduction possible

If pages are missing, contact the university which granted the degree.

Some pages may have indistinct print especially if the original pages were typed with a poor typewriter ribbon or if the university sent us an inferior photocopy.

Reproduction in full or in part of this microform is governed by the Canadian Copyright Act, R.S C. 1970, c. C-30, and subsequent amendments.

AVIS

La qualité de cette microforme dépend grandement de la qualité de la thèse soumise au microfilmage Nous avons tout fait pour assurer une qualité supérieure de reproduction

S'il manque des pages, veuillez communiquer avec l'université qui a conféré le grade

La qualité d'impression de certaines pages peut laisser à désirer, surtout si les pages originales ont été dactylographiées à l'aide d'un ruban usé ou si l'université nous a fait parvenir une photocopie de qualité inférieure

La reproduction, même partielle, de cette microforme est soumise à la Loi canadienne sur le droit d'auteur, SRC 1970, c. C-30, et ses amendements subséquents

The Effects of Monovalent Cations on Yeast Enolase

Roy Musil

A Thesis

in

The Department

of

Chemistry and Biochemistry

Presented in Partial Fulfillment of the Requirements
for the Degree of Master of Science at
Concordia University
Montreal, Quebec, Canada

January, 1992

ISBN 0-315-73632-1

ABSTRACT

The Effects of Monovalent Cations on Yeast Enolase

Roy Musil

Enolase (EC 4.2.1.11) catalyzes the interconversion of 2-phosphoglycerate (PGA) and phosphoenolpyruvate (PEP). The activity of yeast enolase is inhibited by Li^+ and Na^+. Less Li^+ than Na^+ is required to produce a given percentage of inhibition but their patterns of inhibition are the same.

At pH 9.2 inhibition by Li^+ (and Na^+) is partially competitive with respect to Mg^{2+}. At pH 7.1 proton abstraction is partially rate-limiting and the primary kinetic isotope effect on V_{max} is greater than 1.0 (Dinovo & Boyer, 1971). At pH 9.2, the kinetic isotope effect decreases to $\cong$ 1.0, indicating that there has been a change in the rate limiting step(s) of the reaction with proton abstraction no longer being a slow step. A moderate rate of enzyme catalyzed exchange between the C-2 hydrogen of PGA and solvent (50% exchange in remaining PGA after 50% conversion) is observed at this alkaline pH. Li^+ and Na^+ do not affect the rate of exchange. These results are interpreted as follows: Li^+ and Na^+ bind to enolase and decrease the rate of at least one step in the mechanism. At pH 9.2 this step is a fast step in the reaction. The step inhibited by Li^+ cannot be proton abstraction but may be release of product (phosphoenol pyruvate) or Mg^{2+}.

Enolase requires a divalent metal cation for activity and as isolated, the yeast enzyme contains Mg^{2+}. For yeast apoenolase activated by the less effective metal Ni^{2+} at pH 7.1, a kinetic isotope

effect of 1.8 was measured and no significant exchange between the C-2 hydrogen and solvent could be detected. Ni^{2+} cannot be inhibiting the steps following proton abstraction.

For apoenolase bound to the non-activator Ca^{2+} no rate of enzyme catalyzed exchange between C-2 hydrogen of PGA and solvent could be observed. It is likely that the non-activated enzyme is incapable of proton abstraction.

Acknowledgements

I would like to thank Dr. M.J. Kornblatt for her invaluable help and patience during the completion of this project. I would also like to express my gratitude to Dr. L. Colebrook for his willingness to train me on the NMR, assist me in the interpretation of spectra and for allowing me extensive use of the Bruker WP 80SY. Last but not least, I am thoroughly indebted to my wife for putting up with this for much longer than she deserved.

Abbreviations :

AEP	=	3-aminoenolpyruvate-2-phosphate
COSY	=	COrrelated SpectroscopY
DEPT	=	distortionless enhancement by polarization transfer
DSS	=	Sodium 2,2-dimethyl-2-silapentane-5-sulfonate
ϵ	=	molar extinction coefficient
EI	=	enzyme-inhibitor complex
ESI	=	enzyme-substrate-inhibitor complex
EDTA	=	ethylenediaminetetraacetic acid
f_1	=	2nd dimension in COSY spectrum
FID	=	Free Induction Decay
I	=	inhibitor
NMR	=	Nuclear Magnetic Spectroscopy
PGA	=	2-phosphoglycerate
PEP	=	phosphoenolpyruvate
S/N	=	signal/noise ratio
[S]	=	substrate concentration
T_1	=	spin-lattice relaxation time constant
TMA	=	tetramethylammonium ion
v	=	velocity

Table of Contents

List of Figures

List of Figures

List of Tables

Chapter 1: Introduction

The enzyme known as enolase (EC 4.2.1.11, systematic name, 2-phospho-D-glycerate hydroxylase) interconverts the D-isomer of 2-phosphoglycerate (PGA) and phosphoenolpyruvate (PEP).

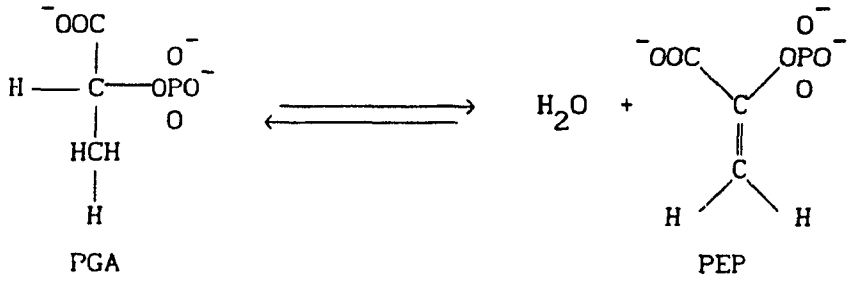

Figure 1.1: Reaction Catalyzed by Enolase

Enolases catalyze the only dehydration reaction in the glycolytic series of reactions and as such are probably found in all organisms that metabolize sugars.

While enolases have been purified from many sources, the best characterized and most extensively studied enolase is that from yeast which has been obtainable in reasonably pure form since 1941.

Yeast enolase is a dimer of approximately 88,000 mol wt. and is composed of two identical subunits (Wold, 1971). The enzyme exhibits an absolute requirement for certain divalent cations for enzymatic activity, of which Mg^{2+} gives the highest activity. Initially, the enzyme binds up to two molesof magnesium upon which a conformational change occurs involving the tertiary but not the secondary structure of the enzyme (Brewer, 1985). Binding of this "conformational" magnesium enables the enzyme to bind up to 2 mol of substrate or competitive inhibitor, though little catalysis occurs. Once the substrate or competitive inhibitor is bound, each subunit can bind one mole of

magnesium and this additional metal produces the actual catalysis, so is called "catalytic" metal. Catalysis may only proceed, however, if the conformational metal ion is one which prefers octahedral co-ordination geometry (Brewer, 1985). A 3rd mole of metal ion/subunit can bind at "inhibitory" sites (Elliot & Brewer, 1980). Certain other divalent metals such as zinc, manganese, nickel or cadmium can provide low levels of activity and thus are called "activators". Others such as calcium, barium or copper allow for no enzymatic activity so are called "nonactivators".

As isolated, yeast enolase contains firmly bound Mg^{2+} (Brewer, 1981). The enzyme may be stripped of its endogenous Mg^{2+} (most simply by dialysis which suggests that the metal is not so tightly bound) and almost any other metal substituted. While not all metal ions activate the enzyme, there is no specificity for those which produce activity. Indeed, Ca^{2+}, Tb^{3+} and Sm^{3+} which do not activate enolase bind tighter than Mg^{2+}.

There is evidence strongly indicating that the conformational metal ion interacts directly with the substrate. When Mn^{2+} is bound at the active site of enolase, two rapidly exchanging water molecules are coordinated to the metal as indicated by the effect of the enolase-Mn^{2+} complex on the lcngitudinal relaxation rate ($1/T_1$) of water protons (Nowak et al., 1973). Nowak et al. have theorized that the conformational metal ion interacts directly with the hydroxyl group on the third carbon of PGA, i.e., the hydroxyl replaces a water molecule of the inner co-ordination sphere of the metal ion (in the reverse reaction, the metal-bound water would add to C-3 of PEP). Their

hypothesis is based on the calculated manganese (II)-phosphorous and manganese (II)-proton distances obtained using ^{1}H- and ^{31}P-NMR and a weak substrate, α-(dihydroxyphosphinylmethyl)-acrylate. Less than two moles of manganese ion per mol of enzyme was present, so Nowak et al. were persumably dealing with conformational metal ions. The calculated distances of approximately 6 Å from the phosphorous and 7.0 ± 0.5 Å from the carbon-bound protons of the substrate were too great for the metal ion to co-ordinate directly with the phosphate or carboxyl group, but were about right for co-ordination with the hydroxyl group of PGA. According to Nowak's model, the -OH of PGA replaces a water coordinated to the Mg^{2+} upon binding to the E-Mg^{2+} complex; upon formation of PEP, the -OH of PGA remains coordinated to Mg^{2+}. These experiments were carried out in 0.5 M KCL.

These authors also obtained evidence suggesting that the substrates and substrate analogues they used allowed 0.3 to 1.0 mol of rapidly exchanging water molecules to remain on the manganese ion. They suggested the analogues "immobilized" 1 mol of metal-bound water so that it exchanged very slowly. This assumes that the co-ordination number of the manganese ion remains the same in the absence of substrate.

Anderson et al. (1984) synthesized a number of reaction intermediate analogues for enolase that have been shown to be good inhibitors of yeast enolase. These compounds are analogues of the aci-form of a carbanion intermediate (a form of the carbanion with the negative charge delocalized to the carboxyl oxygens) and their inhibition of yeast enolase as a function of pH and Mg^{2+} was analyzed in detail. The

binding data support a carbanion mechanism for enolase and suggest that the 3-hydroxyl of PGA is directly coordinated to Mg^{2+} prior to being eliminated to give PEP, as originally postulated by Nowak et al (1973).

All of the tightly bound inhibitors have a trigonal carbon at C-2 and a phosph(on)ate group. It is apparent, however, that a negatively charged group at position C-3 on the substrate can contribute even more to binding strength than a hydroxymethyl group. The most efficient group tested was the ionized hydroxamate of phosphonoacetohydroxamate:

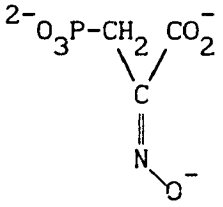

Figure 1.2: Phosphonoacetohydroxamate ion

and the reason for this is most likely that the negatively charged oxygen can assume an out-of-plane position completely isoteric with the 3-hydroxyl of the carbanion intermediate. The nearly three orders of magnitude difference in the binding of 3-hydroxy-2-nitropropyl phosphonate,

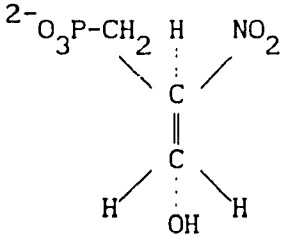

Figure 1.3: 3-hydroxy-2-nitropropyl phosphonate

suggests that Mg^{2+}, which binds very synergistically with substrates and inhibitors, is directly co-ordinated to the 3-hydroxyl group of PGA and of the carbanion intermediate during the reaction.

Nowak et al.'s hypothesis that the hydroxyl on C_3 of the substrate

coordinates directly with the conformational metal ion has been modified by Brewer (1985), however, to accommodate a number of theoretical and experimental difficulties which he has raised:

1) Attempts to show direct interaction between conformational Cu^{2+} and Ni^{2+} and the amino group of the substrate analog AEP,

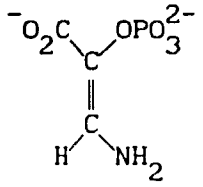

Figure 1.4: 3-aminoenolpyruvate-2-phosphate (AEP)

by looking at differences in the positions of the d-d visible absorption bands using circular dichroism have not been successful (Brewer et al., 1983).

2) Methanolic hydroxyls are generally much poorer ligands to metal ions than water molecules.

3) It is also difficult to explain why AEP binds so much more strongly to the enzyme than the substrate (Brewer & Ellis, 1983) : the amino group of AEP should not interact strongly with Mg^{2+}. Thus, he has proposed that the interaction occurs between a molecule of metal ion-bound water and the substrate / product. Catalysis would involve transfer of protons to and from the bound water molecule, and the substrate.

Nowak et al.(1973) had previously suggested that substrate or analogue "immobilized" one water molecule on conformational Mn^{+2}. They suggested this involved formation of a hydrogen bond with the phosphate of the substrate. In the reverse reaction, a water molecule would have to move into the appropriate orientation between C_3 of PEP and the

metal bound water to produce a transfer to reverse the effect. This scheme places a premium on the orientation of one metal-bound water molecule and hence on the ligand geometry about the metal ion. This is consistent with the observed specificity for divalent cations.

Nowak et al. (1973) could not measure distances to catalytic metal ion in the presence of conformational metal ion using NMR. Brewer and Ellis (1983) speculated, partly from some qualitative effects of Co^{+2} on ^{31}P-NMR spectra of substrate/product, that catalytic metal ion coordinated directly to the phosphate of substrate/product and possibly to the carboxyl as well. The question of whether catalytic metal binds directly to the phosphate of substrate/product has not been settled yet.

All previous proposals regarding metal ion/substrate interaction were made without the knowledge of the 3-D structure of enolase. Recently, the structure of yeast apoenolase was determined (Leiboda et al, 1989) and refined at 2.25 Å (Stec and Lebioda, 1990). The molecule is a dimer of identical subunits related by a crystallographic 2-fold axis of symmetry. Each subunit is built of two domains. The smaller N-terminal domain has an $\alpha + \beta$ structure based on a three - stranded antiparallel meander and four helices. The main domain is an 8-fold $\alpha + \beta$ barrel. The active site is located in a deep cavity at the carboxylic end of the β-barrel (Fig 1.5).

Most recently (Lebioda and Stec, 1991), additional X-ray structural studies have revealed the structure of the ternary yeast enolase-Mg^{2+}-PGA/PEP complex to a resolution of 2.2 Å. It should be noted that the enzyme is active at conditions (pH 5, 50% saturated

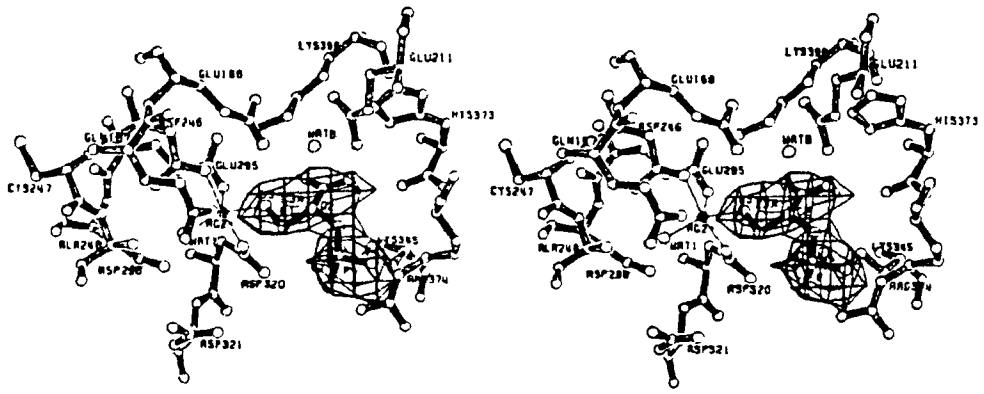

Active site of enolase The electron density, contoured at the 2.5σ level, is from a difference Fourier map phased with a model in which the substrate molecule was omitted The PGA molecule is drawn with heavy lines The water molecule postulated as the catalytic base is denoted as WATB For the product, PEP, the modeled position of carbon-3 is denoted C3A, and the C(2)–C(3A) bond is drawn without shading The modeled position of the product water molecule is somewhat below O(3) (not shown because of overlap) The temperature factors for the active-side residues refined in the 10–20 Å^2 range, and for the substrate, 38–41 Å^2

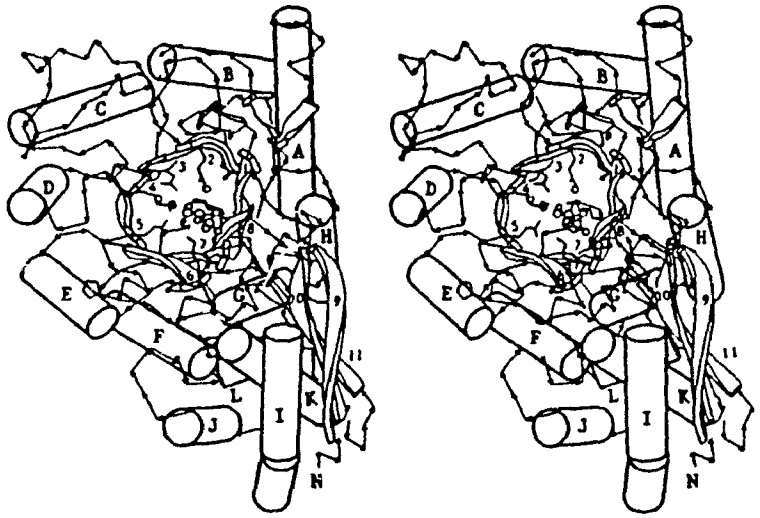

Stereoview of enolase seen approximately along the barrel axis The active site is located in the deep cavity at the carboxylic end of the barrel The position of the conformational metal ion is marked with a filled circle The PGA molecule and two water molecules in the active site are drawn with open circles The main secondary structure elements are denoted according to the previous notation (Lebioda et al., 1989) The sequence of secondary structure elements along the peptide chain is N-9, 10, 11, I, J, K, L, 1, 2, A, B, 3, C, 4, D, 5, E, 6, F, 7, G, 8, and H–COOH The side chains of the active-site residues are drawn as stick models From β-strand 2 branches, Glu168, 3, Asp246, 4, Glu295, 5, Asp320, 6, Lys345, 7, Arg374, and 8, Lys396

Figure 1.5 : Stereoview of Enolase and Active site of Enolase

Taken from Lebioda and Stec, 1991

ammonium sulphate) fairly close to those in the crystals although the K_m values for Mg^{2+} and the substrate are much larger (approx. 100x for each) and the V_{max} is only 5% of the value obtained under standard assay conditions. Leiboda and Stec believe that under these conditions speculations about the mechanism of enolase catalysis may be reasonably drawn.

Surprisingly, the authors have not positively identified any feature in the electron density maps that could be interpreted as the catalytic Mg^{2+} ion. The probable cause of this is that the high ionic strength of the mother liquor increases its dissociation constant to the extent that the electron density of the bound catalytic metal ion is not above the noise level of the map. However, the structure of the ternary complex confirms the trigonal bipyramidal coordination of the conformational metal which was found in the binary enolase-Zn^{2+} complex (Lebioda and Stec, 1989).

Both Zn^{2+} and Mg^{2+} have a strong preference for octahedral coordination when all ligands are oxygen atoms and it was generally assumed that the coordination of the conformational metal was octahedral (Nowak et al., 1973). Thus, it was unexpected that the ligands of Zn^{2+} in the conformational site form an almost regular trigonal bipyramid with two monodentate carboxylic groups of Asp246 and Asp320 in the axial positions while two water molecules and monodentate Glu295 are in the equatorial positions.

Enolase represents the first known trigonal-bipyramidal environment of Mg^{2+} ions (Lebioda and Stec, 1989). Lebioda and Stec have speculated that five coordinated Mg^{2+} or Zn^{2+} are well suited for participation in

enolase catalysis. The metals should strongly polarize the ligand, the water molecule or the hydroxyl group of PGA but the unstable five-fold coordination of the metal ion allows much faster ligand exchange than would be possible with normal octahedral coordination.

In the structures of Ca^{2+} and Sm^{3+} complexes of enolase the metal ion binding site is shifted 0.5 Å from the Zn^{2+} binding site (Lebioda and Stec, 1989). This shift and the larger ionic radii of the non-activating metal ions create sufficient space at the conformational metal ion site to accommodate a third, additional water molecule. The resulting coordination is octahedral.

The X-ray structure indicates that the substrate molecule in the active site has its hydroxyl group coordinated to the Mg^{2+} ion. The carboxylic group interacts with the side chains of His373 and Lys396 and the phosphate group is H-bonded to the guanidinium group of Arg374. A water molecule H-bonded to the carboxylic groups of Glu168 and Glu211 is located at a 2.6 Å distance from carbon-2 of the substrate in the direction of its proton. It has been proposed that this cluster functions as the base abstracting the proton in the catalytic process. The proton is probably transferred, first to the water molecule, then to Glu168, and further to the substrate hydroxyl to form a water molecule. A direct transfer of the proton to Glu168 is certainly a possible alternative that may exist.

The carboxylic group of the substrate is 3.0 Å from one of the δ-atoms of His373. At resolutions achievable with protein crystals, X-ray diffraction experiments do not allow one to distinguish between C and N atoms; the orientation of imidazole and amide moieties is usually

guessed from the environment suitable for the formation of hydrogen bonds. In the structure of apoenolase, Leiboda and Stec have positioned the imidazole ring of His373 so that it forms a hydrogen bond to a water molecule - with an N-O distance refined to 3.0 Å. In the ternary complex, this distance is 3.3 Å while the distance between O(2) of the substrate and $C_{\delta 2}$ of His373 is 3.0 Å. The precision of the structure is insufficient to decide, based on the distances, which of the contacts is actually the H bond; the directions of the N-H bonds are possible in both orientations. The interaction with the carboxylate should be, however, more favorable because of the charges involved. Thus, the authors think it is likely that the side chain of His373 has been flipped 180° and forms a hydrogen bond through its $N_{\delta 1}$ atom to the substrate rather than to the water molecule. This proposed imidazole flip is not based on X-ray diffraction evidence. Nowak et al. (1973) also found two rapidly exchanging water and two or three carboxylic ligands which is in agreement with the crystallographic data.

Another point which should be mentioned with regards to the proposed mechanism based on the crystallographic data is that the positioning of the substrate within the active site is by no means absolute. The electron density at the phosphate position is very high while that of the organic part forms a relatively flat lobe connected to the phosphate density. The carboxylic group and the hydroxyl cannot be distinguished (Lebioda and Stec, 1991). The substrate can be positioned either with the hydroxyl coordinated to the metal ion (Figure 1.6) or with the carboxylic group coordinated to the metal ion in a monodentate fashion.

Figure 1.6 lists the three reaction schemes (Nowak's, Brewer's and Leiboda and Stec's) for the interaction of PGA/PEP with conformational metal at the active site. It would appear that from the weight of the independent evidence that the hydroxyl of the substrate coordinates directly to the conformational metal ion. Yet, the results of the cystallographic data are not so iron clad as to cast aside Brewer's hypothesis. The electron density of the substrate/product at the active site is sufficiently bloated and vague that some averaging of PGA, and the products, PEP and H_2O must be occurring. Thus only very approximate positions can be figured out The question of binding to catalytic metal - in fact even the position of catalytic metal - remains unresolved.

The structures of two inhibitory ternary complexes: yeast enolase-Ca^{2+}-PGA and yeast enolase-Zn^{2+}-PG, have also been determined by X-ray diffraction to 2.2 Å resolution and show two modes of nonproductive binding (Fig. 1.7) by enolase (Lebioda et al., 1991) Phosphoglycolate (PG) is a competitive inhibitor of enolase. In the enolase-Ca^{2+}-PGA complex, the PGA molecule appears to coordinate to the Ca^{2+} ion via the hydroxyl group, similar to the precatalytic complex. The conformation of the PGA molecule though, is different. In the active complex, the organic part of the PGA molecule is planar, much like the product. In the Ca^{2+}-inhibitory complex, the carboxylic group is in an orthonormal conformation. In the inhibitory enolase-Zn^{2+}-PG complex, the PG molecule coordinates to the Zn^{2+} via the carboxylic group in a monodentate mode.

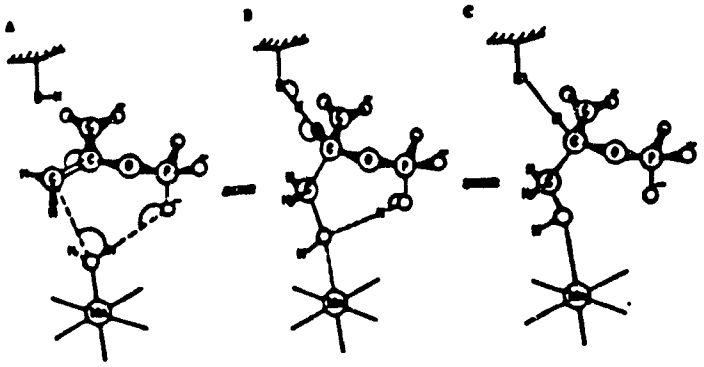

a) Taken from: T. Nowak, A.S. Mildvan and G. Kenyon; Biochemistry, Vol. 12, #9, 1973

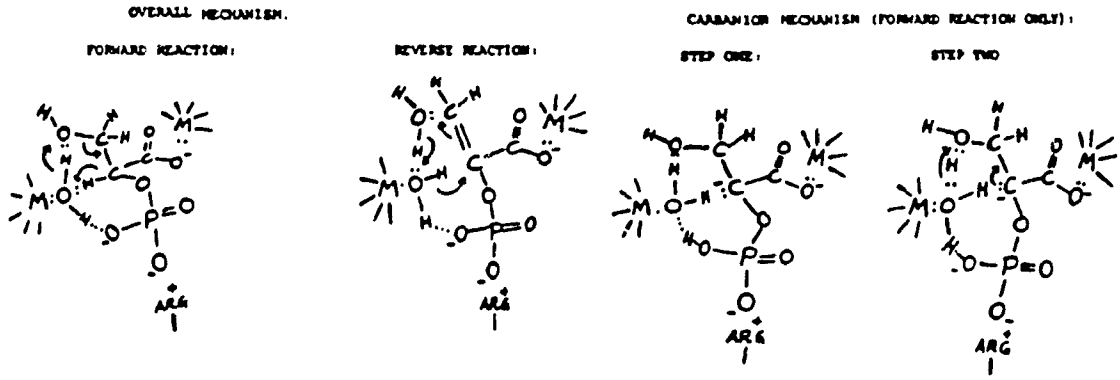

b) Taken From: J.M. Brewer; Febs Letters, Vol. 182, #1, 1985

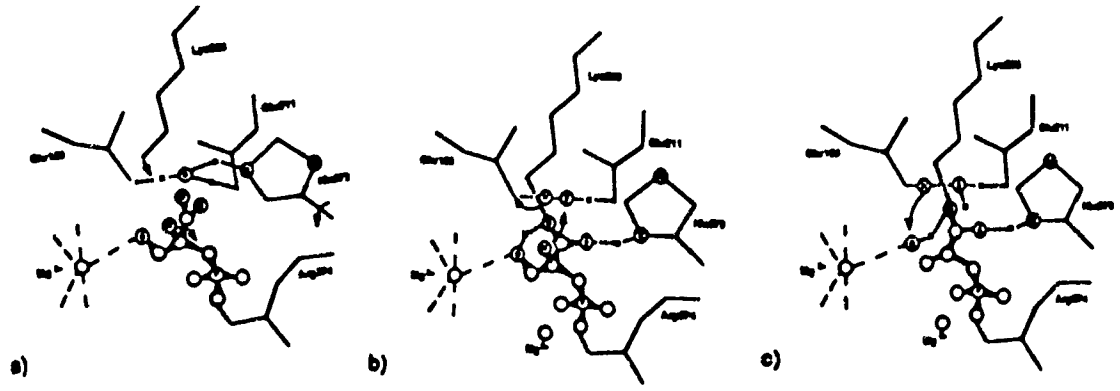

c) Taken From: L. Lebioda and B. Stec; Biochemistry, Vol. 30, 1991

Figure 1.6: 3 Schemes for interaction of conformational metal with substrate/product

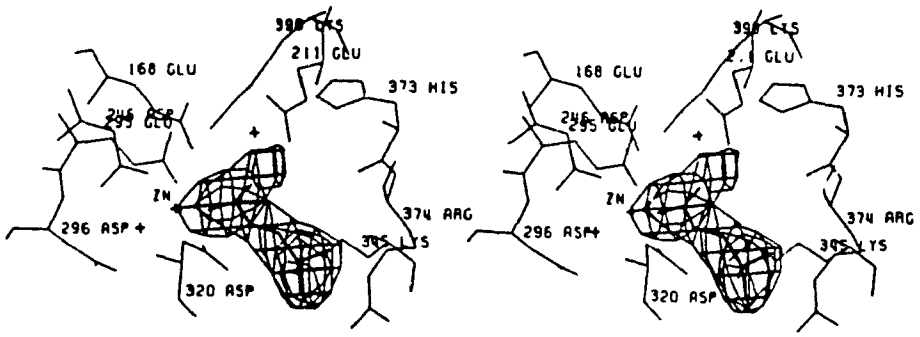

Active site in the enolase-Zn^{2+}-PG complex The inhibitor molecule binds to the metal ion with one of the oxygen atoms The coordination of Zn^{2+} is trigonal bipyramidal, as it is in the binary complex The electron density, contoured at the 2 5σ level, is from an omit difference Fourier map The temperature factors for the inhibitor are in a 37–40-Å^2 range, for the active-site residues in a 10–20-Å^2 range

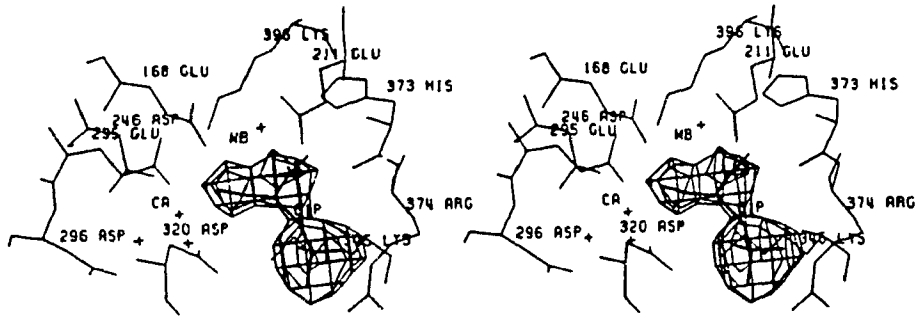

Active site in the enolase–Ca^{2+}-PGA complex The electron density, from a difference Fourier map contoured at the 2.0σ level, indicates that the carboxylic group is perpendicular to the plane of the carbon atoms The water molecule postulated as the base in the precatalytic complex, WB, is not in a position to interact with the proton on C(2), and neither is Glu168 The temperature factors for the PGA molecule are in a 40–44 Å^2 range for the active site residues in a 10–20-Å^2 range

Figure 1.7 : Active Site in the enolase-Ca^{2+}-PGA complex and in the enolase-Zn^{2+}-PG complex. Taken from Lebioda et al., 1991

For both inhibitory complexes, just as in the case for the active ternary complex with Mg^{2+}, there was no electron density that could be assigned to the catalytic metal. For the active ternary complex, substrate/product binding is accompanied by large movements of loops Ser36-His43 and Ser158-Gly162 (Lebioda and Stec, 1991). While the role of these loop movements have not yet been determined, in both inhibitory complexes the conformational changes in the flexible loops do not take place. The authors think that this conformational transition is crucial for the formation of the catalytic metal ion binding site. Until the catalytic metal binding site is found in the active complex, however, this hypothesis will remain weak.

It is generally accepted that the enolase reaction proceeds through a carbanion (C-2 proton off first) mechanism (see Fig 1.6 and Fig 1.8). In isotope exchange experiments involving ^{3}H, ^{2}H, ^{18}O and ^{14}C, Dinovo and Boyer (1971) established the relative rates of isotopic exchanges at chemical equilibrium shown in Table 1.1.

Table 1.1

Isotopic Exchange Rates at Chemical Equilibrium (enolase)
pH 7.8 and 25mM $MgCl_2$

Isotopic Exchange	Relative Rate
[^{2}H]-PGA $\rightleftharpoons$ [^{2}H]-H_2O	1.9
[^{18}O]-PGA $\rightleftharpoons$ [^{18}O]-H_2O	1.3
[^{14}C]-PGA $\rightleftharpoons$ [^{14}C]-PEP	1.0

With [^{3}H]-PGA, the relative rate of exchange with H_2O was 0.9,

suggesting that a kinetic isotope selection is occurring and allowing one to calculate the anticipated [^{1}H]-PGA $\rightleftharpoons$ H_2O exchange from the following two equations (Dinovo and Boyer, 1971):

$$K_H/K_T = (K_D/K_T)^{3.26}$$

$$K_H/K_T = (K_H/K_D)^{1.44}$$

On this relative scale, the protonic exchange rate from C-2 of PGA to H_2O is 12 establishing this as the fastest partial exchange. This evidence is consonant with a carbanionic species forming during enzyme catalyzed dehydration. On the other hand, with 2-[^{2}H]-PGA there was no deuterium kinetic isotope effect on V_{max} of PEP formation (the overall reaction), in contrast to the large discrimination in the exchange reaction. This suggests that the proton abstraction at C-2 of PGA, involved in overall PEP formation is a fast step in catalysis. Boyer suggested the following sequence, in which the carbanion is formed in a quasi-equilibrium step, to account for the experimental data :

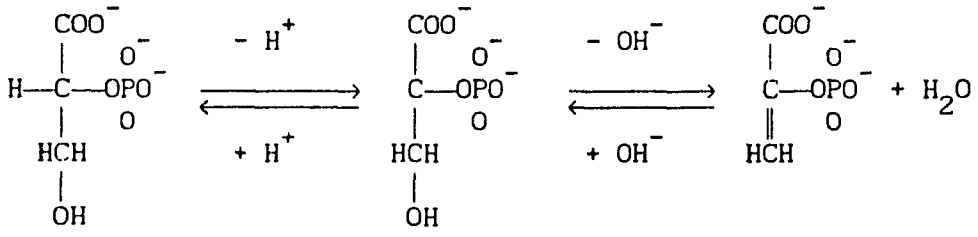

Figure 1.8: Mechanism of the Dehydration Reaction Catalyzed by Enolase

In actuality the simplest mechanism for enolase must include at

least four steps (Kornblatt and Musil, 1990) :

1) binding of Mg^{2+}, PGA and a second Mg^{2+} to the enzyme

2) proton abstraction

3) loss of OH^- to produce PEP

4) release of both Mg^{2+} ions and PEP from the enzyme

There is a pronounced inverse secondary isotope effect of the C-3 hydrogens on the rate of formation of PGA from PEP (C-3 ^3H gives higher rates of PGA formation than does C-3 ^1H) showing that the rate limiting step for the reverse reaction must be the addition of OH^- to the enol double bond. The only reasonable precursor of the sp^3 hybridization of C-3 is the transition state involved in the OH^- addition, and the sp^3-sp^2 transition is thus proposed to be the rate limiting step.

Dinovo and Boyer (1971) studied isotope rates at equilibrium with rabbit muscle enolase and did not observe a primary isotope effect at 2-[^2H]-PGA on the dehydration rate. Shen and Westhead (1973) observed a substantial isotope effect in the reaction catalyzed by both rabbit muscle and yeast enolase. This effect is markedly dependent on both pH and activating cation. Thus, there is not a serious discrepancy between the two studies since Dinovo and Boyer looked for the isotope effect at pH 7.8 where the effect is relatively small.

The maximum isotope effect seen with Mg^{2+} yeast enolase was more than a third of the "theoretical" isotope effect which would be seen if carbon-hydrogen bond scission completely dominated the rate of dehydration.

Substitution of Mn^{2+} or Co^{2+} leads to a considerably lower catalytic

efficiency and a marked lowering of the primary isotope effect. At pH 7.8 the relative rates wih Mg^{2+}, Mn^{2+} and Co^{2+} were determined to be : 1.0 : 0.4 : .1 and the respective isotope effects were : 2.1 : 1.6 : 1.0. So with Mg^{2+} or Mn^{2+} proton removal is somewhat limiting, except at alkaline pH's. At alkaline pH's or at all pH's with the cobalt enzyme, hydroxyl removal or possibly product release are limiting.

Shen and Westhead continued and extended some unpublished experiments begun with Dr. A. Kowalsky in 1961. In these experiments the proton nuclear magnetic resonance spectra of PGA and PEP were observed in D_2O during dehydration of PGA by yeast enolase. Since all the protons of the substrate and product are observable, it is possible to measure the rate of exchange of the C-2 proton of PGA by its disappearance relative to the C-3 protons. According to the mechanism shown in Figure 1.8, exchange of the hydrogen on C-2 of PGA with solvent can occur by a reversal of steps prior to product release. The extent of hydrogen exchange will be determined by the partitioning of the carbanion between product formation and reprotonation to form PGA.

The NMR data shows very slow exchange (not over 5% at 50% conversion) at pH 7.2 where the isotope effect is strong. This correlates with other results which paint a picture of nearly rate-limiting proton abstraction. At pH 9.2 where it was found that there is almost no isotope effect, a moderate rate of exchange was observed (50% exchange in remaining PGA at 50% conversion). If no exchange were found, the results would show either sequestration of the removed proton by the enzyme or that catalysis proceeds by a carbonium ion mechanism in which a slow hydroxyl ion removal precedes rapid

proton removal and product release.

Shen and Westhead's data clearly show that as the pH is raised steps other than hydrogen abstraction increasingly dominate the catalytic rate. At low pH the proton abstraction step is slow enough to restrict the dehydration rate but as pH increases, the latter steps of the reaction (hydroxyl ion removal and product release) decrease in rate and limit the dehyration process.

This present work aims to expand upon the use of NMR as a technique for probing the mechanism of yeast enolase. Specifically, to determine the effects of monovalent cations (particularly Li^+) on the dehydration process catalyzed by enolase activated with Mg^{2+}. Yeast enolase has previously been shown to be inhibited by Li^+ and Na^+ (Kornblatt & Klugerman, 1988). Through the use of steady - state kinetics, measurements of the primary kinetic isotope effect and measurements of hydrogen exchange with solvent, the mechanism of inhibition will be assessed.

The technique of measuring the rate of exchange of the C-2 proton of PGA relative to its C-3 protons will also be applied to apo-enolase activated by Ni^{2+} and Ca^{2+}. It has been postulated that the less effective metals decrease the efficiency of either hydroxyl ion removal or product release or both (Shen & Westhead, 1973). If proton abstraction is no longer the rate limiting step in the reaction mechanism; that is, if hydroxyl ion removal or product release or both have been significantly inhibited, an increase in the exchange rate between solvent and the hydrogen of carbon-2 of PGA will be seen. In addition to proton NMR analysis, a preliminary look at ^{18}O isotope

exchange as determined by ^{13}C NMR will be reported. ^{18}O exerts an isotope effect on ^{13}C NMR signals of directly bonded carbon atoms which results in an upfield shift of the ^{13}C resonance signal of otherwise comparable atoms bearing ^{16}O oxygen. The ^{18}O isotope effect has been demonstrated to be a general phenomena (Risely & Van Etten, 1981). If the reaction catalyzed by yeast enolase proceeds in $H_2{}^{18}O$, ^{18}O may be incorporated into PGA by a reversal of steps prior to product release. If product release is slowed a greater proportion of ^{18}O will be incorporated and measured as an increase in peak size at its upfield shift position. If hydroxyl ion removal is inhibited there will be no change in ^{18}O accumulation.

Chapter 2 Materials and Methods

2.1 Materials

Yeast enolase was purchased from Sigma (USA). Yeast apo - enzyme was prepared by dialysis against EDTA via the method of Brewer and Weber (1965). 2-[^{2}H]-PGA was prepared enzymatically according to the method of Shen and Westhead (1973) with slight modifications by Kornblatt and Klugerman (1989). Enolase preparations were stored concentrated in 50% glycerol at -20°C in plastic vials. The trisodium salt of PGA and the tricyclohexylammonium salt of PEP were purchased from Boehringer Mannheim. "Puriss" grade KCl, NaCl, and LiCl were purchased from Fluka Chemie ; tetra-methylammonium chloride (98%) from Alfa Products,. "100%" deuterium oxide and $H_2{}^{18}O$ (97%) were purchased from Merck Sharpe and Dohme.

2.2 Methodology

Enolase activity was measured at 25°C by following the production of PEP at 240nm. In order to determine the concentration of 2-[^{2}H]-PGA prepared enzymatically, it was necessary to convert PEP to lactate by the addition of ADP, NADH, pyruvate kinase and lactate dehydrogenase. PGA production was then assayed for by following the utilization of NADH at 340nm. All assays were performed in duplicate, in 50mM imidazole, pH 7.1 or in 25mM borate, pH 9.2, with concentrations of salts, magnesium acetate and PGA as stated. When measuring the primary kinetic isotope effect , all assays (2-H-PGA and 2-^{2}H-PGA) contained 8mM TMA chloride.

The extinction coefficient of PEP varies with pH as well as with the concentrations of KCl and magnesium ions (Wold and Ballou, 1957),

therefore the results of pH studies were analyzed using values of ϵ determined in the buffer used.

Residual metal ion bound to the apoenzyme was assayed from the 296nm absorbance change in the enzyme produced by adding excess EDTA, then excess magnesium (Figure 2.1). An increase in absorption, with a peak at 296nm and a shoulder at 288 occurs when excess magnesium is added to an EDTA-saturated enzyme solution (Brewer & Weber, 1965). The use of enzymatic activity for assays of residual metal ions is a poor method for determining metal ion content, both because many divalent metals do not activate enolase and because up to two moles of Mg^{2+} ion can bind without producing much activity (Brewer, 1981). The 296nm absorbance change seems to be a reasonable index of total metal ion content since most divalent metal ions appear to produce it and it has been labeled as the "best" method for routine use (Brewer, 1981).

The observed absorption change suggests that the polarity of the environment of one or more tryptophans is decreased when Mg^{2+} is added. The change itself is small, and the difference spectrum is buffer dependent, depending on interaction of the apoenzyme with tris base.

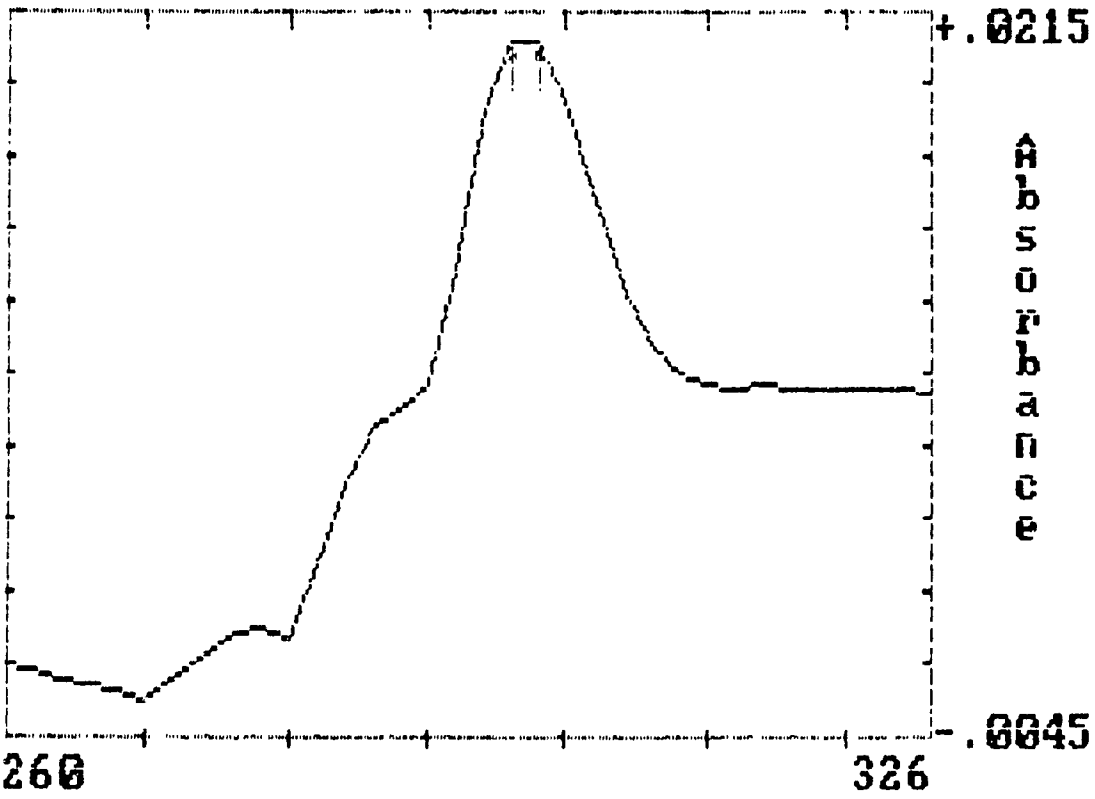

Figure 2.1 Ultraviolet difference absorption spectrum of yeast enolase (.4mg/ml) in the presence of 14mM Mg^{2+}, pH 7.1, 25°C , 25mM Tris (sample) and presence of 1mM EDTA (reference).

For the proton NMR experiments, enzymatic assays were performed in "100" D_2O and at various times after the addition of enolase, aliquots were removed and the reaction quenched by the addition of EDTA in a four times molar excess to the Mg^{2+} concentration of the given assay. Samples were lyophilized, re-dissolved in D_2O and pulsed Fourier transform spectra were then run.

The pulsed Fourier transform proton spectra were obtained either at 25mM PGA on a Bruker WP 80SY (due to the low sensitivity of the instrument) using 5mm NMR tubes or at 5mM PGA, in the case of the apoenolase studies, on a Bruker WH-400 NMR. The spectra were referenced against DSS with no linebroadening or Gaussian multiplication applied. The spectral window was set at 10ppm. When using the 80MHz instrument 40 FIDs per spectrum were acquired, while on the 400 MHz NMR, 16 scans were collected. To ensure the proper identification of the C-2 and C-3 proton signals a standard COSY experiment (Sanders & Hunter, 1987) was performed on the WP 80SY NMR. The COSY employed a 256 x 256 data block with one level of zero filling in f_1.

The C-2 and C-3 protons both give well resolved multiplets but because of the peak overlap within each individual multiplet it was deemed inappropriate to use integration as a means of quantitation (Sanders and Hunter, 1987). This overlap makes the beginning and ending of the integrals very much an arbitrary affair and in the case of the relatively small peaks of the C-2 septet, may significantly alter their total area. An initial problem which also precluded the use of peak areas for the C-2-[H] PGA signal was the fact that the septet was located at the edge of the large solvent peak. The lack of a flat

baseline (which prohibits integration) was, however, largely overcome through the lyophilization procedure. This being the case, the peak height of the most prominent peak in each multiplet was used for quantitation.

It is absolutely essential that the data be collected under conditions which allow uniform recovery of all signals that are to have their heights (or areas) measured. Thus, when π / 2 recovery pulses are being used , a relaxation delay of at least 5 times T_1 must be allowed between successive pulses (Sanders and Hunter, 1987). The most common method of measuring spin-lattice relaxation rates, an inversion recovery sequence, was therefore performed with a line broadening of 0.5 - using the pulse sequence :

$$\pi \; - \; t_D \; - \; \pi / 2 \; - \; \text{Acquire}$$

where ; $\pi = \pi$ pulse

t_D = is a delay under the control of the operator

$\pi / 2 = \pi / 2$ pulse

From the null points of Figure 2.2, it can be seen that the C-2 proton has a T_1 of approx. 3.0 seconds while the C-3 protons have a T_1 of .6 seconds. A relaxation delay of 17 seconds was then employed.

The ^{13}C NMR experiments were performed at 25mM PGA and 10mM Mg^{2+}. All spectra were obtained at 100MHz using 10mm NMR tubes. For each spectra, 1292 FID's were averaged into a 16K data block. The enzymatic assays were carried out in 50% $H_2{}^{18}O$ and after the addition of enolase, the reaction was quenched by the addition of 40mM EDTA .

The strategy for identifying the ^{13}C peaks involved :

1) a proton broadband decoupled ^{13}C NMR spectrum, to count

nonequivalent carbon atoms

2) a Distortionless enhancement by polarization transfer :DEPT which generates C, CH, CH_2 and CH_3 subspectra allowing for the determination of CH_n multiplicities.

2.3 Data Analysis

Kinetic data were analyzed by the kinfit program using an unweighted fit (Knack and Rohm, 1981).

Peak heights were converted to concentrations using a standard curve (figure 2.3). The data are reported as the ratio of C-2-[H] PGA to total PGA (C-3-[H]-PGA) vs. percent reaction (determined from the change in total PGA concentration).

Figure 2.2 : The inversion Recovery Signals from PGA

The value of t_D is given beside each trace

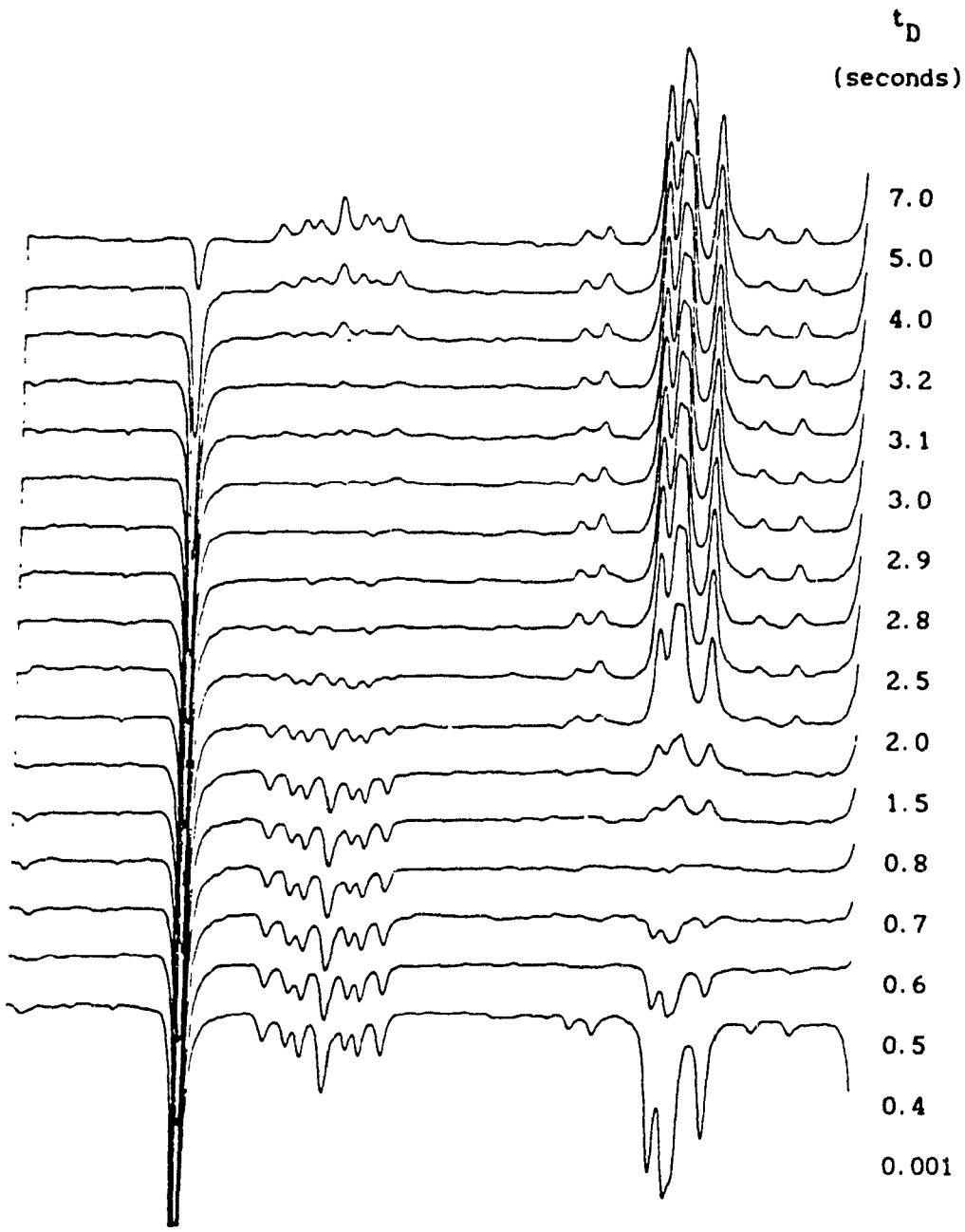

Figure 2.3 : Standard Curve for Determination of PGA Concentration
Signal Height (cm) vs. Conc. PGA (mM)

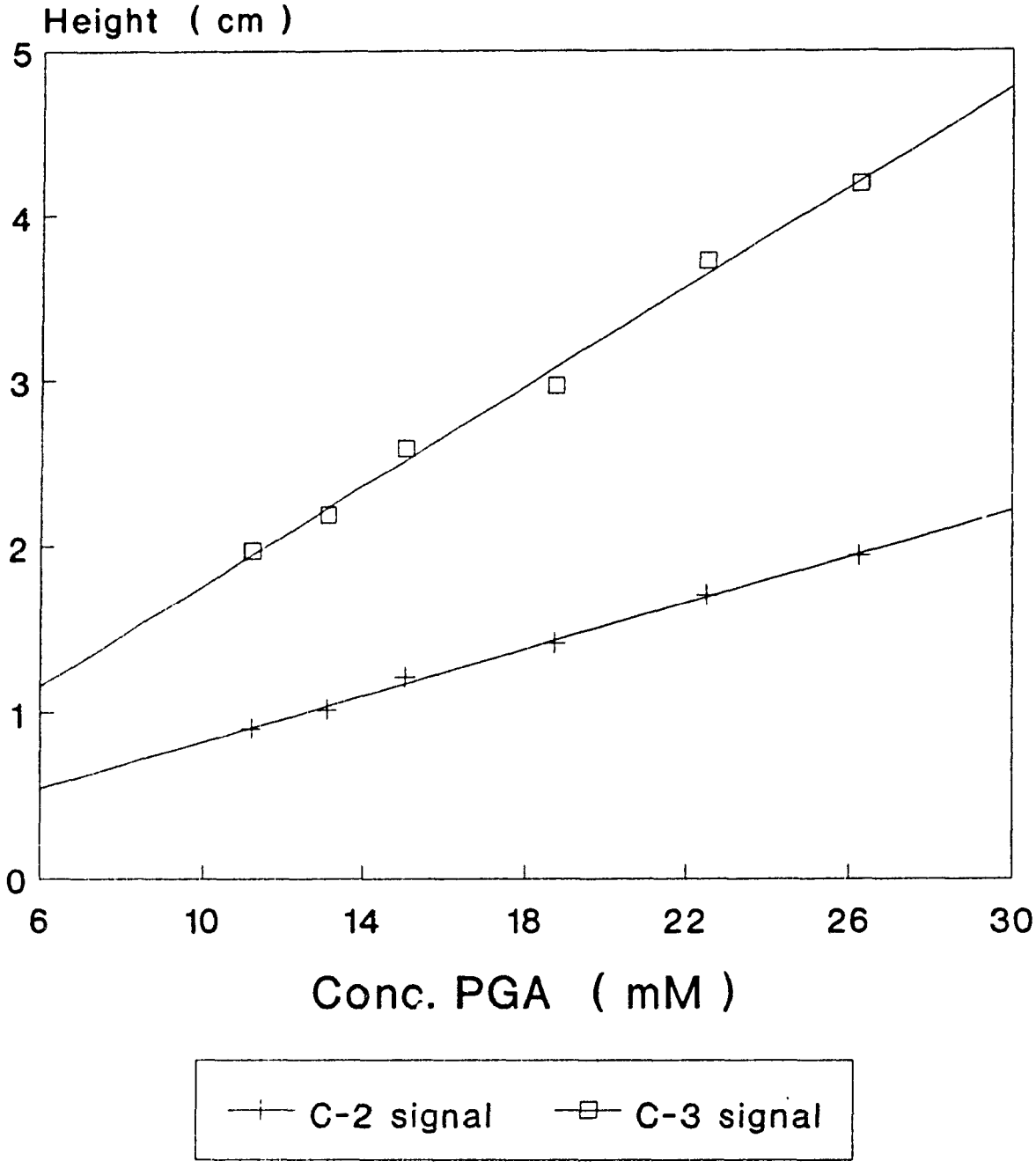

Chapter 3 Physical Parameters Affecting The Activity of Yeast enolase

3.1 : Introduction

The initial aim of this work was to use NMR to monitor proton abstraction as a probe of the effects of monovalent cations (specifically Li^+) on yeast enolase. For this aim to be achieved, it is necessary to conduct experiments at pH 9.2 and at a sufficiently high substrate concentration so as to produce "reasonable" NMR spectra. At pH 9.2 a moderate rate of exchange for the C-2 PGA proton relative to the C-3 protons has been previously shown (Shen & Westhead, 1973).

By conducting the present experiments at this alkaline pH we may observe an effect on the rate of exchange in the presence of monovalent cations. If only the proton abstraction step is inhibited, we would expect a slower rate of exchange. Inhibition of hydroxyl ion removal, the step which immediately follows proton abstraction, would lead to a greater incorporation of deuterium into the substrate and hence a greater observed rate of exchange. Inhibition of product release (PEP and/or Mg^{2+}) should not affect the rate of exchange.

To this end, an essential first step must include a characterization of the effects of monovalent cations, high pH, and high substrate concentration on the enzyme.

Experiments were also performed at pH 7.1 with Mg^{2+}, where no exchange was observed by NMR. This may be particularly interesting in the cases of divalent metal substitution in apoenolase. If a significant exchange rate is measured, we can conclude that steps subsequent to proton abstraction are inhibited, thus causing the lower activity.

The pH optimum for yeast enolase is 7.7 and the optimum concentration of Mg^{2+} for activity is 1mM (Wold, 1971). Much of the earlier work on the effects of monovalent cations - comparing their effects on rabbit brain enolase isozymes and yeast enolase - was conducted at pH 7.1.(Kornblatt & Klugerman, 1989)

3.2 : Effects of pH and PGA Concentration

Figure 3.1 shows the initial characterization of conditions under which the NMR experiments are to be performed. It can be seen that under low substrate concentrations there is approximately 70 % loss of activity in going from pH 7.1 to pH 9.2. This drop in activity may be attributed at least in part to the decrease in the hydroxyl ion removal and product release steps of the reaction.

The inhibitory effects of alkaline pH become much less pronounced as the substrate concentration is increased. NMR experiments on the WP 80SY were refined to the point that 25mM PGA was sufficient for well resolved spectra. At this concentration there is approximately 25 % difference in the activities between the two pH's, but the overall inhibition is continuing to increase. At infinitely high concentrations of PGA at both pH's, an asymtopic low level of activity appears to be attained.

An obvious explanation for the decrease in activity at high PGA concentrations is the phenomenon of substrate inhibition. A second molecule of substrate binds to give an ES_2 complex that is catalytically inactive (Fersht, 1985). If, in a simple Michaelis-Menten mechanism, the second dissociation constant is K'_s then :

Figure 3.1:
Relative Activity vs. PGA (mM)
at pH 7.1 & pH 9.2 and 1mM Mg(II)

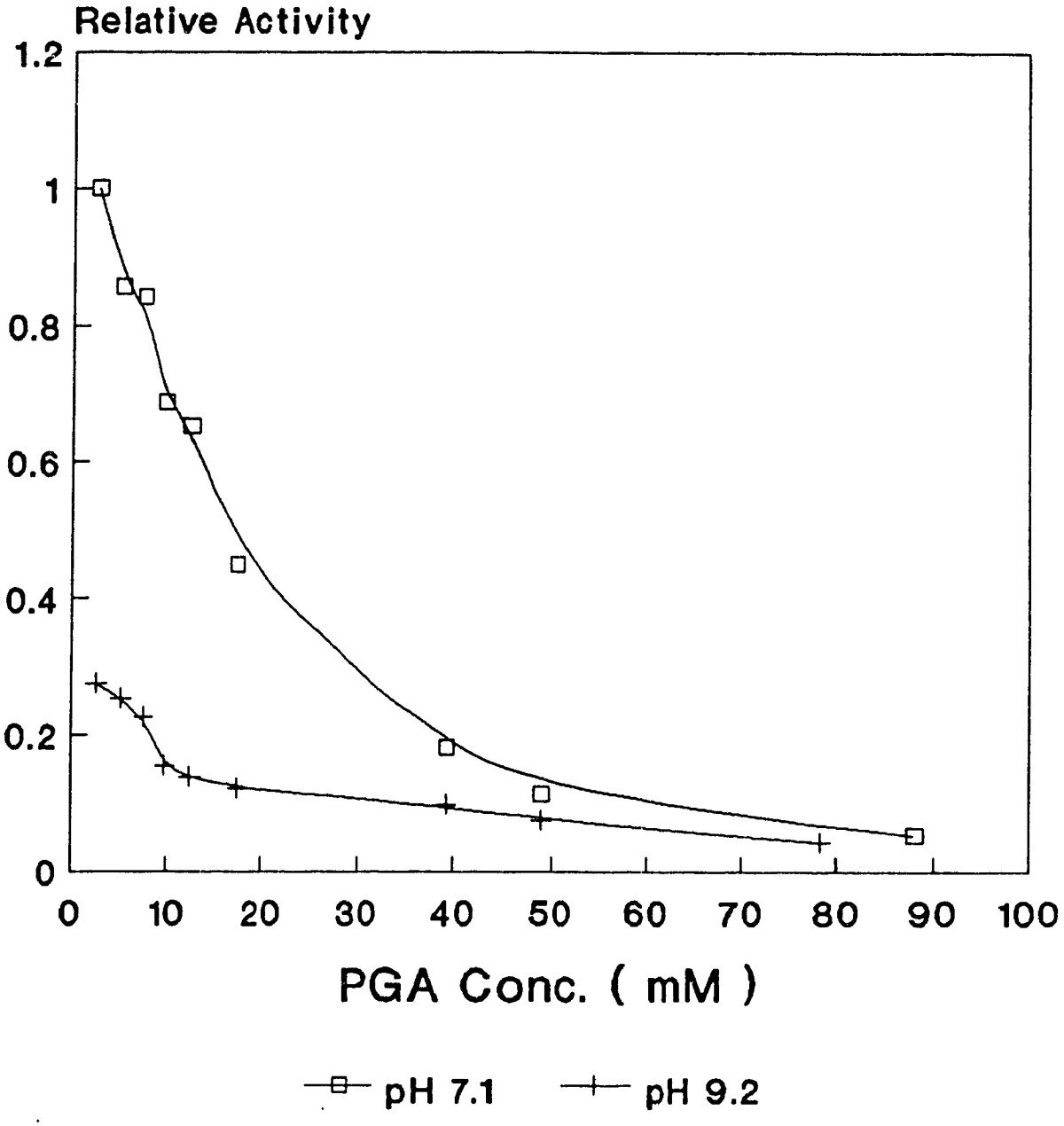

Figure 3.2 :
Relative Activity vs. Mg(II) (mM)
at pH 7.1 & pH 9.2

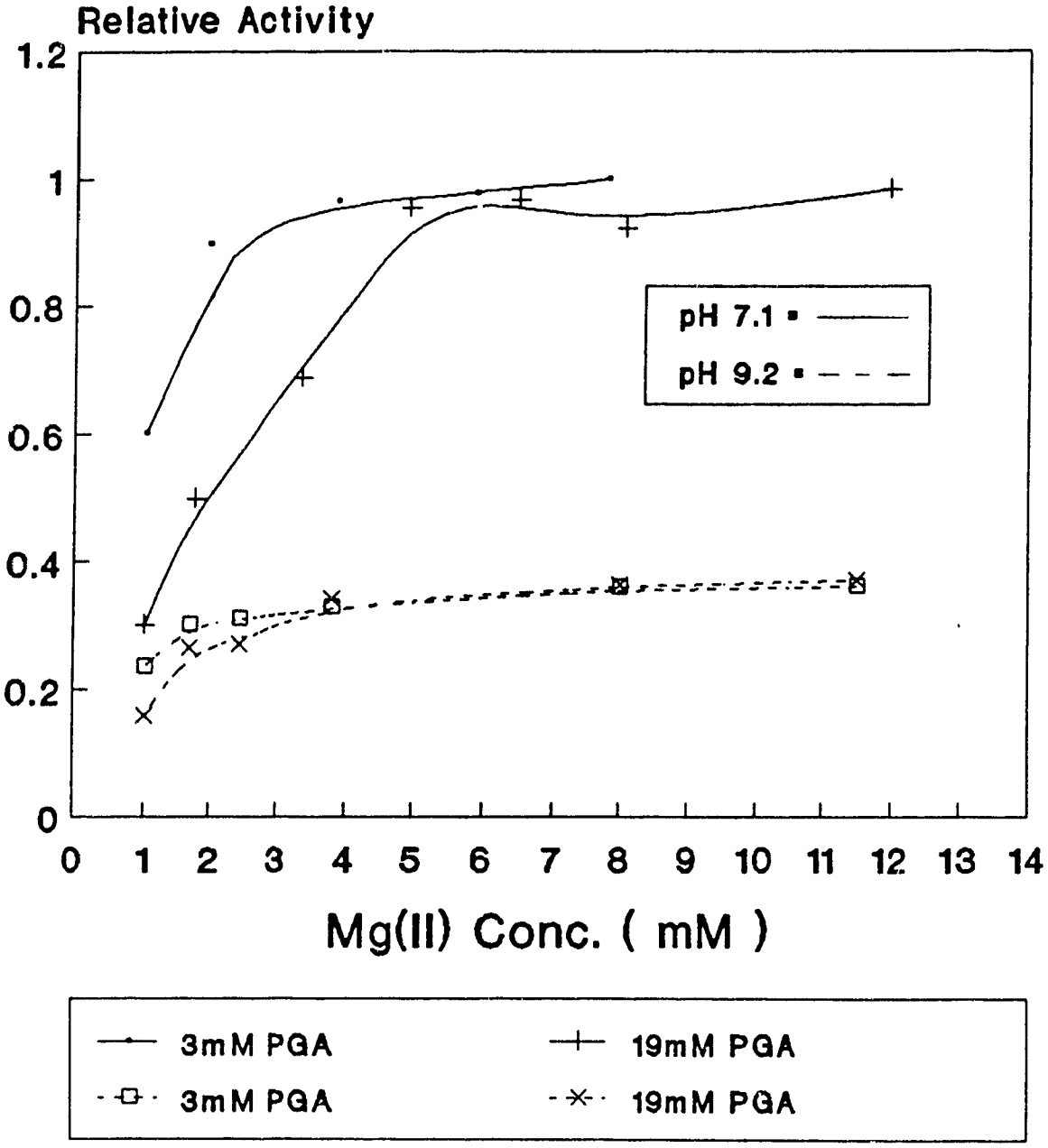

$$v = \frac{[E]_0 [S] k_{cat}}{K_s + [S] + [S]^2/K'_s} \qquad \text{(eqn. 1)}$$

At low concentrations of [S], the rate is given by the usual equation : $v = [E]_0 [S] k_{cat} / K_s$ (eqn. 2)

But as [S] increases, there is first a maximum value of v followed by a decrease.

The activity of all enolases is inhibited by excess Mg^{2+}, but its structural basis is not well understood (Brewer, 1985). Part of the reason why mammalian enolases have a slightly lower pH optimum for activity than does yeast enolase (pH 6.7 to pH 7.1 vs. pH 7.7) is the inhibition of activity by Mg^{2+} at higher pH. A preliminary investigation was performed to determine the effects of Mg^{2+} on activity under conditions of high substrate concentration. The results from Figure 3.2 indicate that a major factor contributing to the decrease in activity at high PGA concentrations is not an excess of Mg^{2+}, but an apparent lack of saturating Mg^{2+} (ie : an increase in K_m for Mg^{2+}). These results also show that the observed loss of activity is due to more than substrate inhibition. In fact, much of the effects attributed to substrate inhibition are eliminated by increasing Mg^{2+}. Thus we must address the question of whether or not Mg^{2+} binding to PGA at high substrate concentrations is no longer negligible. We may in fact have a significant concentration of Mg^{2+}-PGA complex and very little free Mg^{2+}, which would account for the observed decrease in activity.

Wold and Ballou (1957) have previously calculated binding constants for complexes of PGA with several metals, including

magnesium. The binding constants were estimated according to the method of Smith and Alberty, who showed that at constant ionic strength the shift in the apparent dissociation constant of an acid, caused by the addition of metal, is related to the metal concentration and the binding constant for the acid-metal complex in the following way:

$$pK_a' \text{ (no metal)} - pK_a' \text{ (metal)} = \log (1 + D [M]),$$

where ; D = binding constant or stability constant

M = metal concentration

Using a binding constant value of 280 l per mole (Wold and Ballou, 1957) for the complex of PGA with magnesium we may proceed to make estimates on the amount of free Mg^{2+} and substrate in solution. Table 3.1 was generated under the assumption of a one to one binding stoichiometry for the Mg^{2+}-PGA complex and neglects the effects of any other buffer components.

Table 3.1: Binding of Mg^{2+} to PGA in Solution

Magnesium added to assay (mM)	PGA added to assay (mM)	Free Mg^{2+} (mM)	Free PGA (mM)	Mg^{2+}-PGA complex (mM
1	1	.81	.81	.19
1	19	.16	18.16	.84
10	19	2.4	11.4	7.6

Even using such rough estimates it is readily apparent that under low substrate concentrations, Mg^{2+} binding is fairly negligible but at concentrations of 19mM (as used in Fig. 3.2) it is a very serious concern. At 19mM PGA and 1mM Mg^{2+} concentrations the amount of free Mg^{2+} available to bind with enolase becomes significantly reduced.

Increasing the concentration of Mg^{2+} to compensate for its complexing to PGA allows us to return to high levels of enolase activity. The apparent lack of saturating levels of Mg^{2+} can therfore be attributed to low levels of free Mg^{2+} in solution due to Mg^{2+}-PGA complex formation at high substrate concentrations

The need to isolate the contributions of Mg^{2+} and high PGA concentration on the activity of enolase led to a through examination of the kinetic parameters involved (Chapter 4)

3.3 : Effects of Monovalent Cations

The effects of NaCl, LiCl, KCl and tetramethylammonium (TMA)chloride on the reaction rate of the standard assay of 1mM Mg^{2+} in borate buffer , pH 9.2 ,are shown in Figure 3.3. TMA is used as an ionic strength control, since, due to its large size as compared to the other ions, we would not expect it to bind to a site on the protein. Effects of TMA are thus interpreted as being only due to the increased ionic strength.

Li^+ produces a maximum loss of activity at a much lower concentration compared to the other monovalent cations. It has been previously suggested by Kornblatt & Klugerman (1989) that a correlation exists between the size of the ion and its effects on activity. Smaller ions (Na^+, Li^+) inhibit the activity with the smallest ion being the best inhibitor. The effective radii (pm) of the monovalent cations used are :

Li^+ = 74 Na^+ = 102 K^+ = 138

50% loss of activity appears at 50mM Li^+ while 225mM Na^+ is required for the same decrease. By comparison, only 10mM Li^+ is needed

Figure 3.3 : Effects of LiCl, T.M.A, KCl & NaCl on Yeast Enolase Activity at pH 9.2 ; 1mM PGA & 1mM Mg(II)

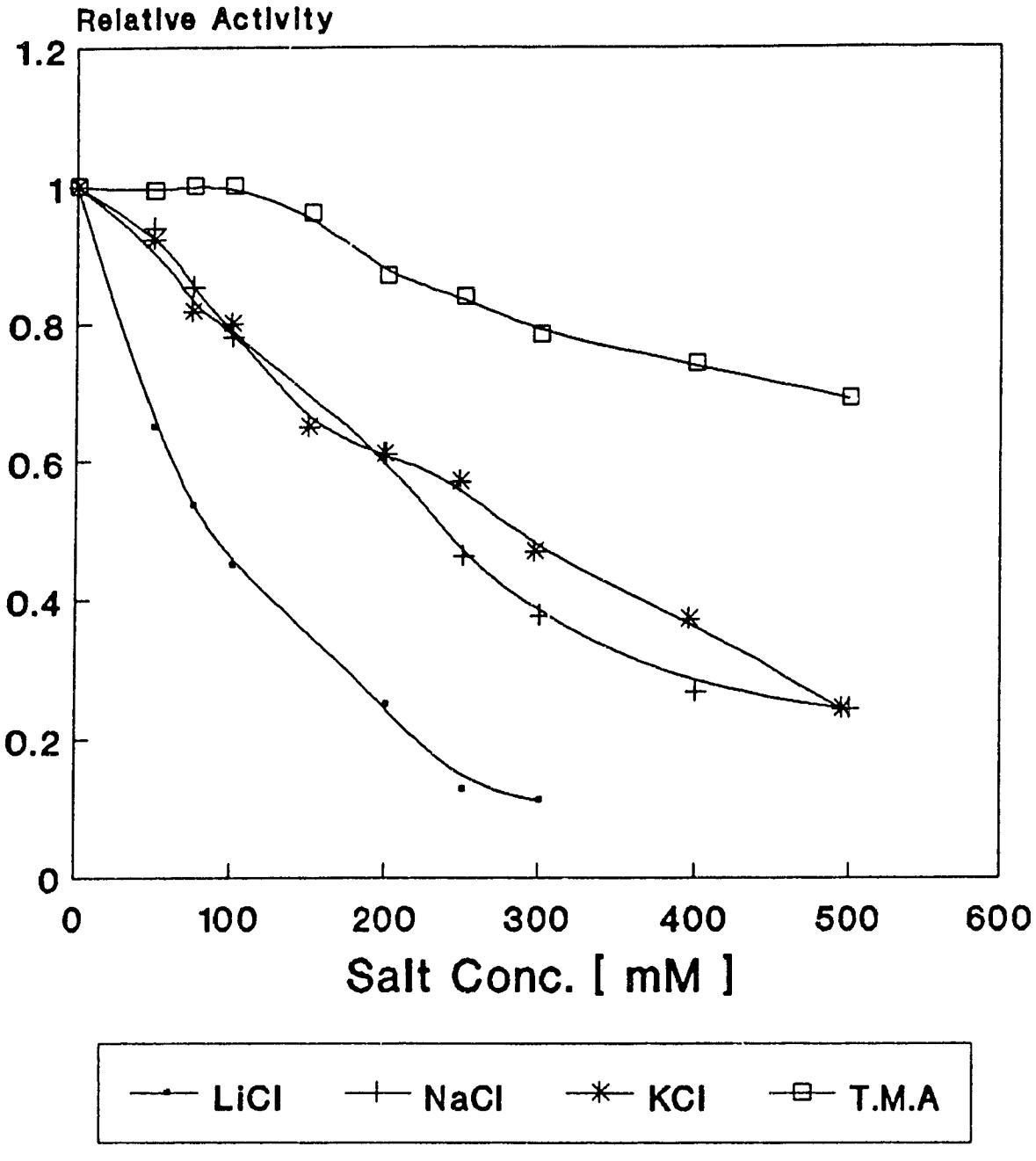

Figure 3.4 : Inhibition by Monovalent Cations under NMR Conditions : 25mM PGA & 10mM Mg(II), pH 9.2

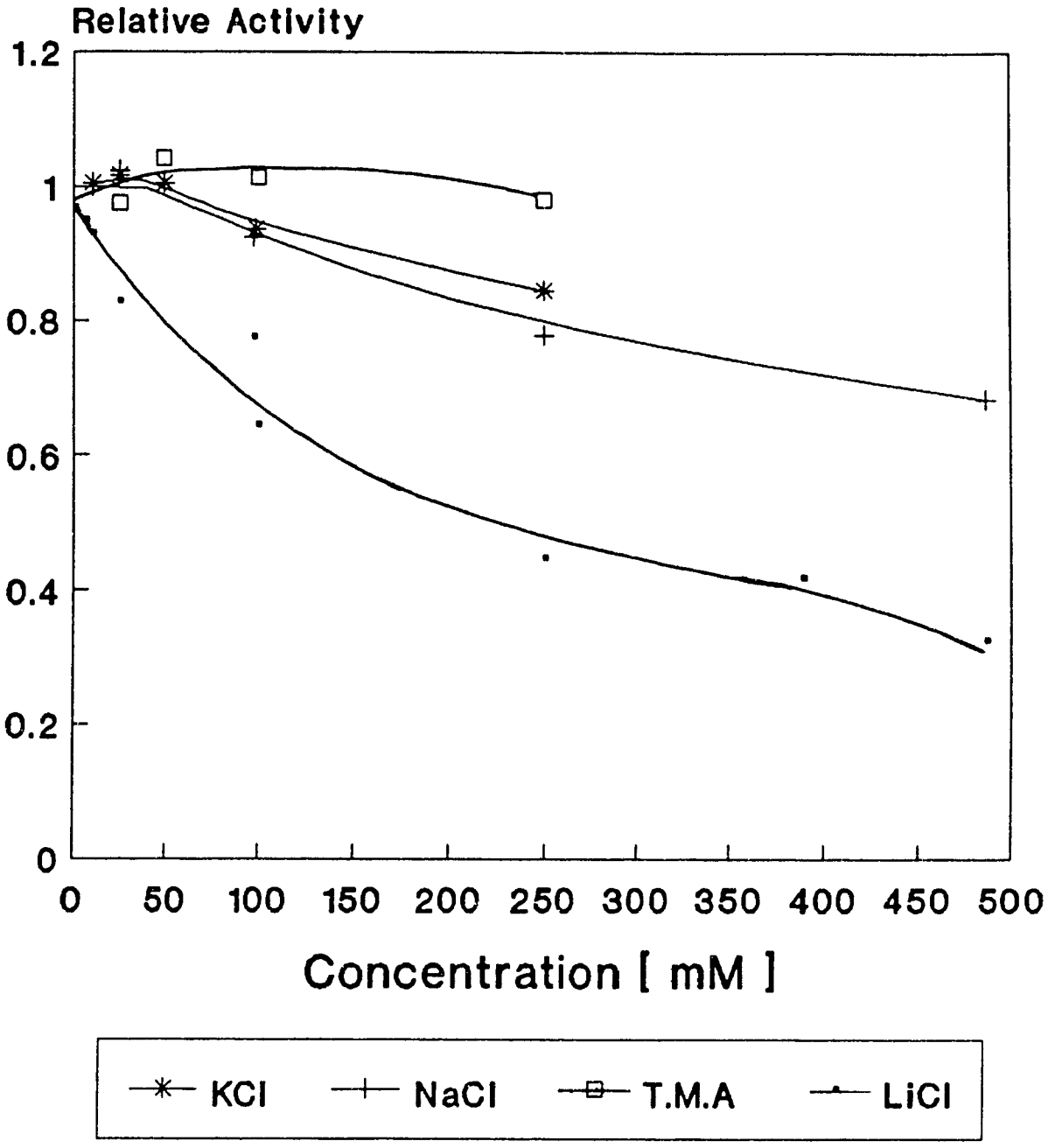

to achieve the same decrease in activity at pH 7.1.(Kornblatt & Musil, 1990)

All ions were tested as their Cl^- salts. The difference in magnitude of inhibition is evidence that the results shown in Figure 3.3 are due to M^+ inhibition and not due to Cl^- or the increased ionic strength.

Because we ultimately wish to monitor the effects of these cations by measuring the rate of exchange of the C-2 proton of PGA relative to its C-3 protons (through the use of NMR), it would be useful to study the effects of monovalent cations under conditions employed for NMR. It can be seen from Figure 3.4 that at 25mM PGA and 10mM Mg^{2+} (a concentration found saturating) the inhibitory effects of the monovalent cations are less pronounced. 50% inhibition now requires 225mM Li^+ or >500mM Na^+. However, only 10mM Li^+ is needed to decrease activity by 8% in comparison to the relatively high concentrations of Na^+ required to observe a similar effect on activity. It was decided that the effects of Li^+ would be the focus of this study. The results with TMA suggest that high ionic strength also effects activity. By being able to use a comparatively low concentration of inhibitor, the added effects of high ionic strength can be neglected. Detailed studies on the mechanism of Li^+ inhibition were then performed.

3.4 : Activation of Apoenolase

All apoenolase studies were performed at pH 7.1 and 5mM PGA since NMR experiments on the Bruker 400 MHz would also have to be conducted at this same concentration. The advantage of using the high field instrument is that a lower PGA concentration is required to produce quality spectra, thus eliminating some possible problems caused by high

ionic strength.

Figure 3.5 shows the activity of apoenolase activated by a variety of divalent cations. The order for relative maximum rates is :

$Mg^{2+} > Zn^{2+} > Mn^{2+} > Cd^{2+} > Ni^{2+} > Ca^{2+}$

This order for metal activation is consistent with previous studies (Brewer, 1981). No catalysis is expected to occur with Ca^{2+} since it produces binding but no distortion at the conformational site on the enzyme (Brewer, 1981). Table 3.2 gives the optimum concentrations for the metals tested and the relative maximum rates achieved with each :

Table 3.2 : Concentrations (mM) of Divalent Metal for Activation of Apoenolase at pH 7.1 and 5mM PGA

(above these concentrations inhibition is observed by the activating metal species)

Metal	Metal. Conc. (mM)	Relative Max. Activity *
Zn^{2+}	1 **	.411
Mn^{2+}	.19	.345
Cd^{2+}	1.9	.064
Ni^{2+}	.5	.049
Ca^{2+}	no activation	

* Relative Activity compared to activation with 1mM Mg^{2+} under the same conditions

** Maximum concentration tested

Figure 3.5 : Relative Activity vs. Divalent Cation Concentration for Apoenolase at 5mM PGA ; pH 7.1

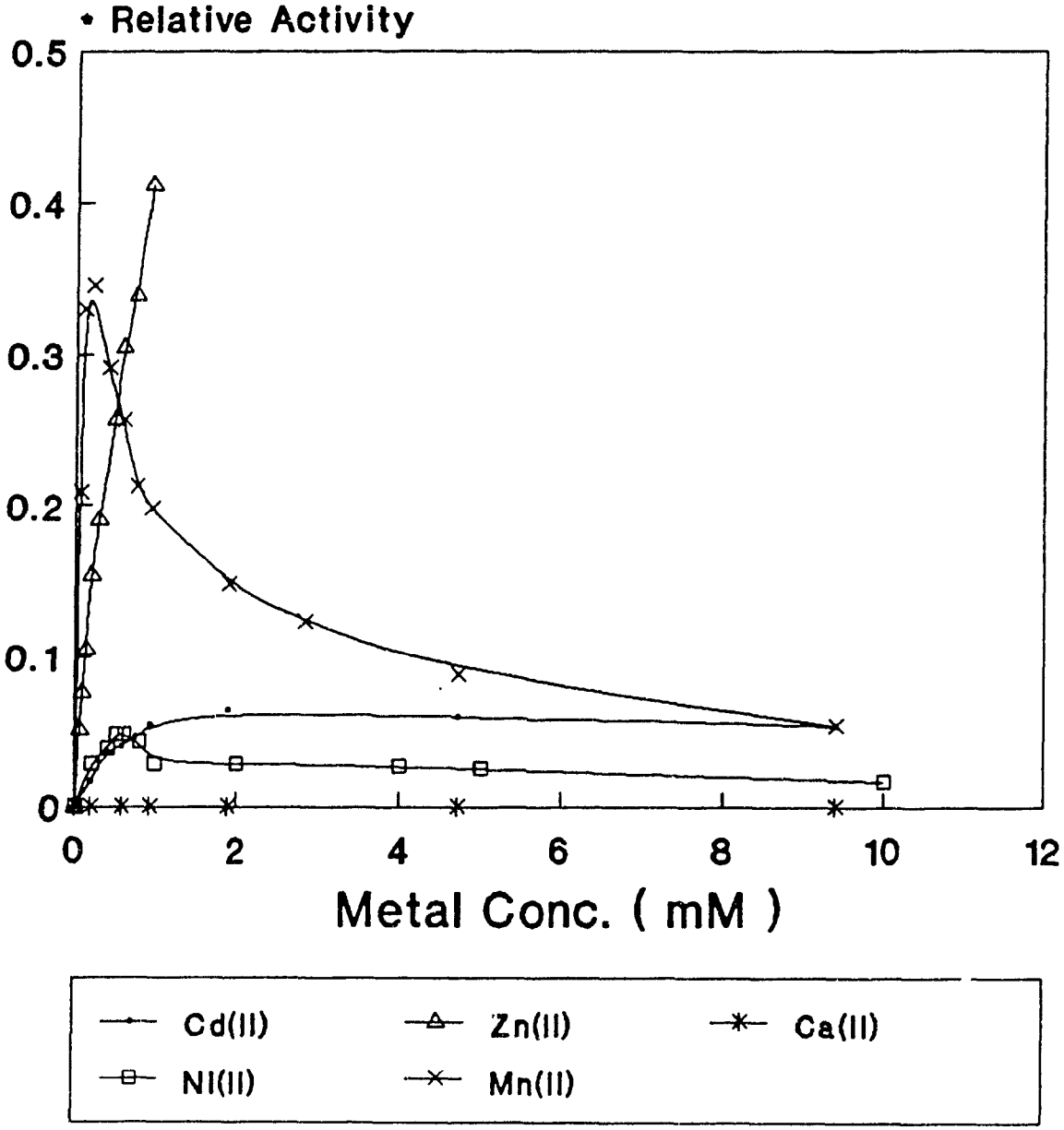

• Relative Activity compared to activation with 1mM Mg(II) under same conditions

The order of the activating metals reflects not only the effect of the metal ion in promoting the rate limiting step but probably also the effect of binding metal ion at "inhibitory" sites. It has long been known that a sufficient excess of any metal ion inhibits the enzyme. This may occur through simple chelation of the substrate by the metal ion , but kinetic studies have shown that metal ions may inhibit by binding to the enzyme, either at a separate site or in a different way from catalytic metal (Wold & Ballou, 1957).

The buffer system used contains 50mM imidazole. Imidazole has been used to obtain optimal activity with enolase, along with a number of other enzymes, and has been implicated in providing protection of the inhibitory site (Elliot & Brewer, 1980). Studies on Zn^{2+} activated enolase (10nM enolase, pH 7.7, 1mM $ZnCl_2$ and 0.04 M and/or 0.16 M imidazole-HCl, pH 7.7) appear to show that the amine buffer removes the inhibition by chelation of zinc from an inhibitory site on enolase : the metal-amine complex does not bind to the enzyme.

The level of activity produced is roughly inversely proportional to the electronegativity of the metal ion and proportional to the readiness of the metal ion to form complexes which are other than octahedral (Brewer, 1985). If one compares the effective radii (pm) of metal ions in octahedral coordination : Mg^{2+} = 72

Zn^{2+} = 74

Mn^{2+} = 67

Cd^{2+} = 95

Ni^{2+} = 61

Ca^{2+} = 100 (Bell, 1977)

It is apparent that there is just a narrow range of metal radii around an optimum of 72 pm for maximum activation.

For this present study, it was thought that it would be of the most interest to concentrate on the divalent metals which produced the lowest activity (Ni^{2+} & Ca^{2+}). We could then determine if the lack of observed activity is due to a retardation of a particular step in the reaction mechanism.

Chapter 4 Determination of Kinetic Parameters. Type of Inhibition

4.1 : Introduction

Since the results with TMA^+ suggest that high ionic strength also affects the kinetics, and high concentrations of Na^+ are required to observe an effect, more detailed studies were performed with Li^+.

Although less Li^+ than Na^+ is required to produce a given percent inhibition, the pattern of inhibition at pH 7.1 has been found to be the same for both (Kornblatt and Musil, 1990). When PGA is held constant and $[Mg^{2+}]$ is varied, Li^+ affects both V_{max} and K_m. The Lineweaver-Burke plots at varying $[Li^+]$ intersect at a common point with the inhibition pattern appearing to be "mixed" (Segal, 1975).

The most common type of "mixed" inhibition has the enzyme with inhibitor bound inactive: as the concentration of inhibitor is increased, V_{max} approaches zero. Another type of inhibition is hyperbolic (partial) mixed-type inhibition where the inhibitor and the variable substrate, Mg^{2+}, are both bound to the enzyme but the complex is active. The binding of inhibitor increases K_m for Mg^{2+} and decreases the activity: a plot of V_{max} vs. [Inh] approaches a limiting value.

It has been concluded (Kornblatt and Musil, 1990) that at pH 7.1, inhibition by Li^+ is consistent with the hyperbolic (partial) mixed type mechanism. This conclusion is supported by kinetic isotope effects which demonstrate that enzyme with Li^+ bound is active.

In chapter 3 it was shown that monovalent cations, alkaline pH and high substrate concentration all have an affect on yeast enolase activity. The effects of monovalent cations, most specifically Li^+, and

high substrate concentration at pH 9.2 were further examined so as to determine the type or mechanism of inhibition present under conditions to be used for NMR exchange experiments.

4.2 : Effects of PGA

Figure 4.1 and Table 4.1 illustrate the effects of increasing PGA concentration on the kinetic parameters of K_m and V_{max} at pH 9.2 when Mg^{2+} is the variable substrate. It should be noted that for all Lineweaver-Burke plots, 1/V is plotted against the inverse of the total concentration of Mg^{2+} added to the assay and not the "free" Mg^{2+} in solution which may be estimated (as in Table 3.1) by using the binding constant for the Mg^{2+}-PGA complex as calculated by Wold and Ballou (1957). As can be seen from Table 4.1, the primary effect of increasing the PGA concentration is to increase the K_m for Mg^{2+}.

This drastic increase of K_m for Mg^{2+} at 25mM PGA agrees with the previous finding that at high PGA concentrations it is a lack of saturating Mg^{2+} which accounts, at least partially, for the decrease in reaction rate. The results indicate that under NMR conditons (pH 9.2 and 25mM PGA) used to observe exchange , the effects of Mg^{2+} must be considered and the effects of high substrate concentration must be compensated for.

A question which has to be addressed is whether the kinetic effects observed under high PGA concentrations are solely attributable to high ionic strength effects or are specific to the substrate.

Figure 4.1 : Lineweaver - Burke Plot
Determination of Km & Vmax
pH 9.2 & Increasing PGA concentration

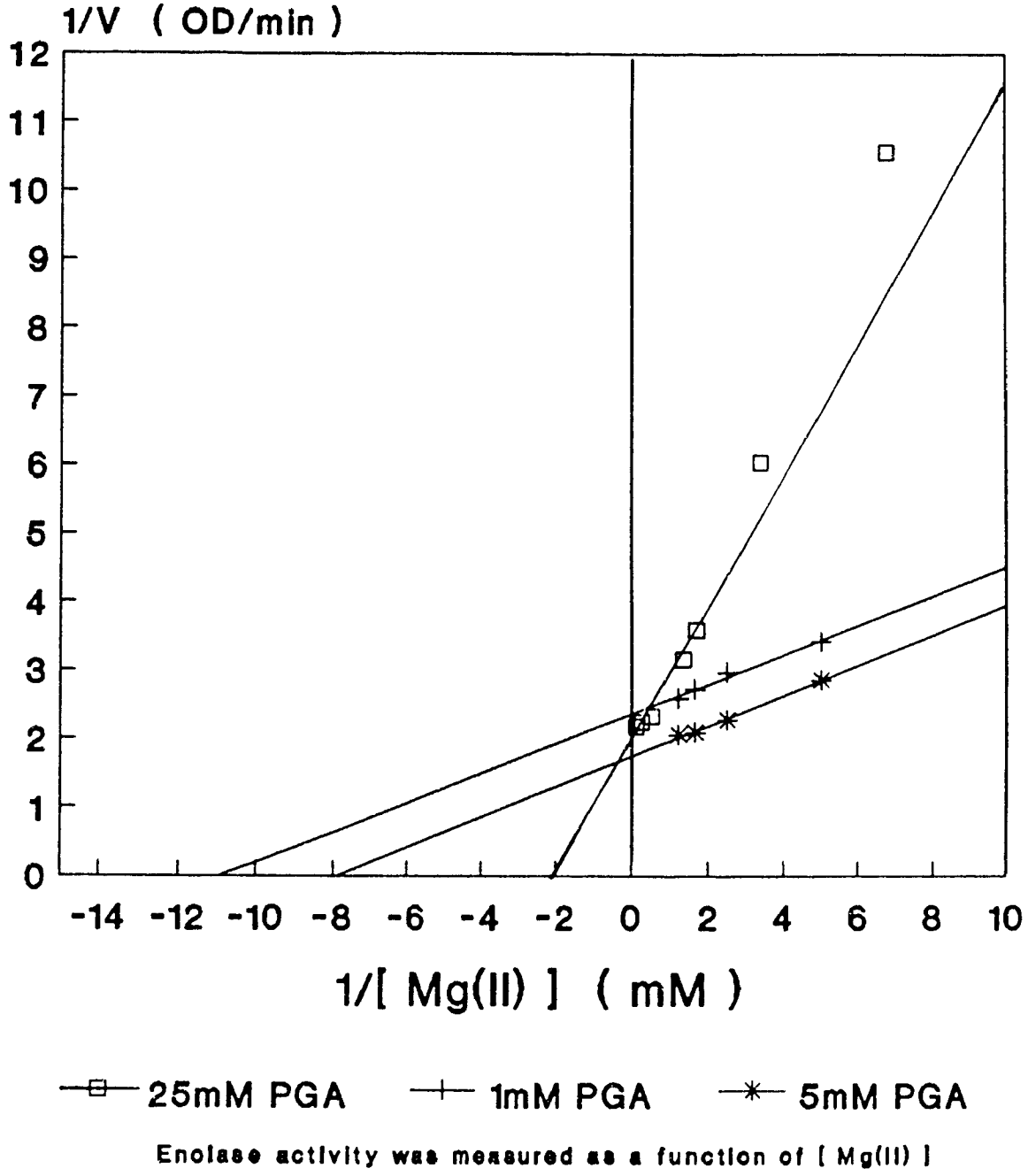

Enolase activity was measured as a function of [Mg(II)]

Table 4.1 : Effects of Increasing PGA Concentration at pH 9.2

PGA conc. (mM)	K_m for Mg^{2+} (mM)	V_{max} (relative)
1.00	.097 ± .014	1.00 ± 2.80%
5.00	.123 ± .010	1.33 ± 1.88%
25.00	.487 ± .057	1.19 ± 3.58%

4.3 : Effects of Monovalent Cations

Table 4.2 : Effects of Monovalent Cations on Kinetic Parameters at pH 9.2 and 1mM PGA

Cation	K_m (mM) (Mg^{+2})	V_{max} (relative)
no salt	0.091 ± .011	1.000 ± 3.22%
25mM K^+	0.197 ± .027	0.987 ± 5.04%
25mM Na^+	0.273 ± .050	1.011 ± 6.71%
25mM TMA^+	0.142 ± .006	0.931 ± 3.27%
10mM Li^+	0.226 ± .017	1.000 ± 6.36%
25mM Li^+	0.390 ± .043	1.044 ± 5.56%

Table 4.3 : Effects of Monovalent Cations on Kinetic Parameters at pH 9.2 and 25mM PGA

Cation	K_m (mM) (Mg^{+2})	V_{max} (relative)
no salt	0.487 ± .057	1.000 ± 3.52%
25mM K^+	0.972 ± .063	0.988 ± 7.67%
25mM Na^+	0.952 ± .141	1.019 ± 9.20%
25mM TMA^+	0.628 ± .140	0.979 ± 6.16%
10mM Li^+	0.628 ± .039	0.994 ± 5.69%
25mM Li^+	1.516 ± .231	1.013 ± 9.45%

Figure 4.2 : Lineweaver - Burke Plot Inhibition of Enolase Activity by 25mM Na(I), K(I), TMA at pH 9.2 & 1mM PGA

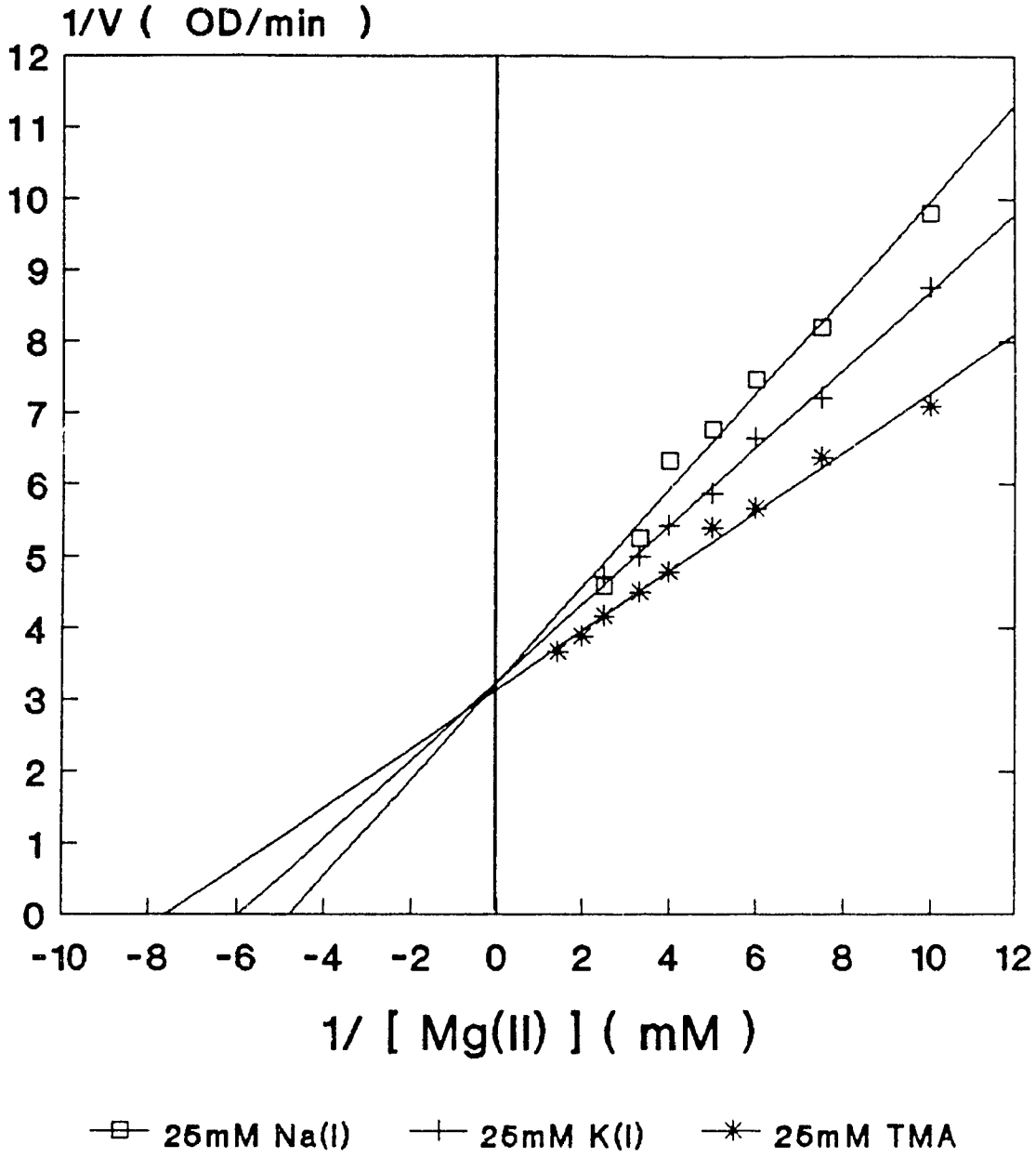

Enolase activity was measured as a function of [Mg(II)]

Figure 4.3 : Lineweaver - Burke Plot
Inhibition of Enolase Activity by Li(I)
pH 9.2 & 1mM PGA

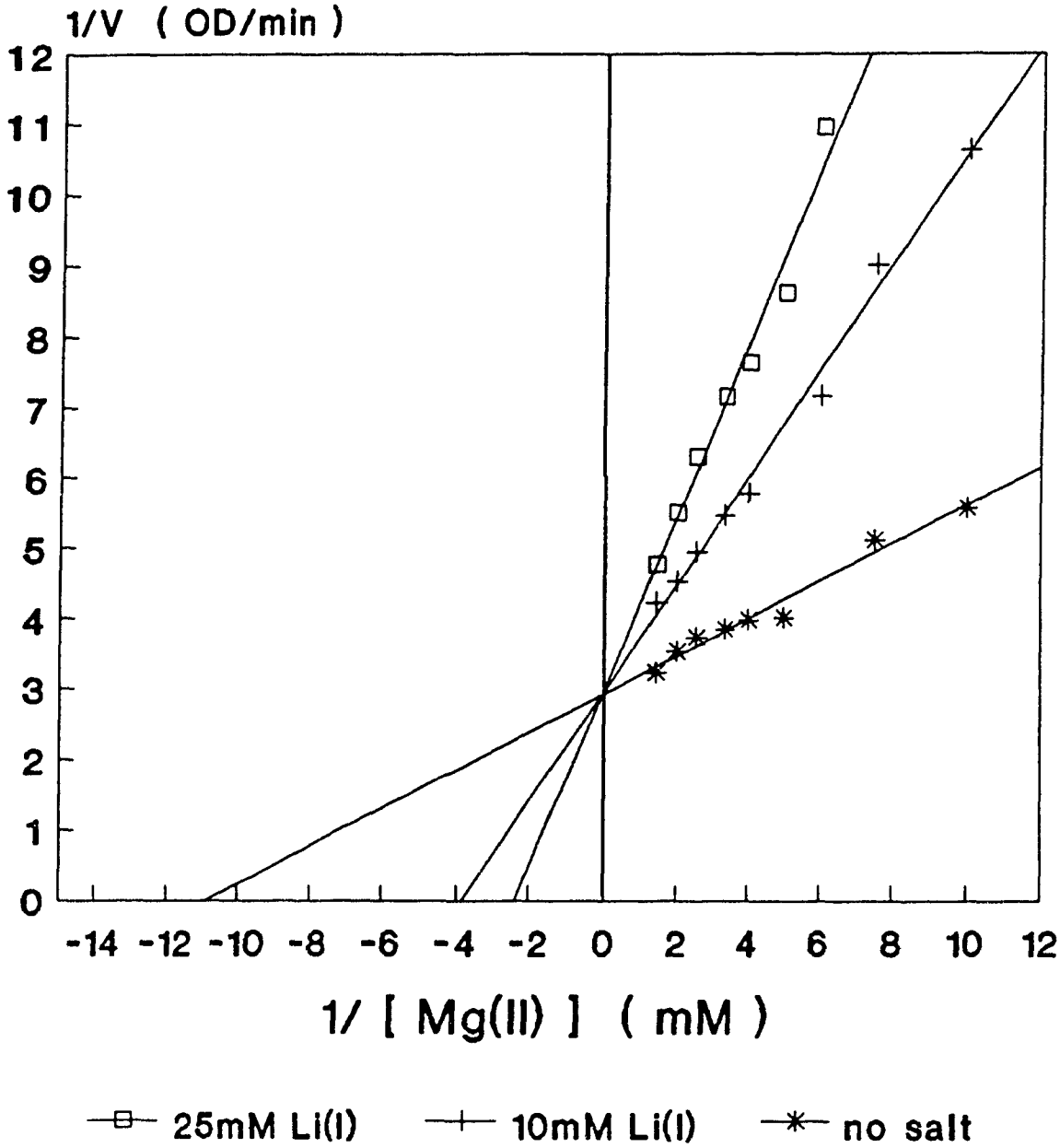

Enolase activity was measured as a function of [Mg(II)]

Figure 4.4 : Lineweaver - Burke Plot
Inhibition of enolase activity by 25mM Na(I), K(I), TMA at pH 9.2 & 25mM PGA

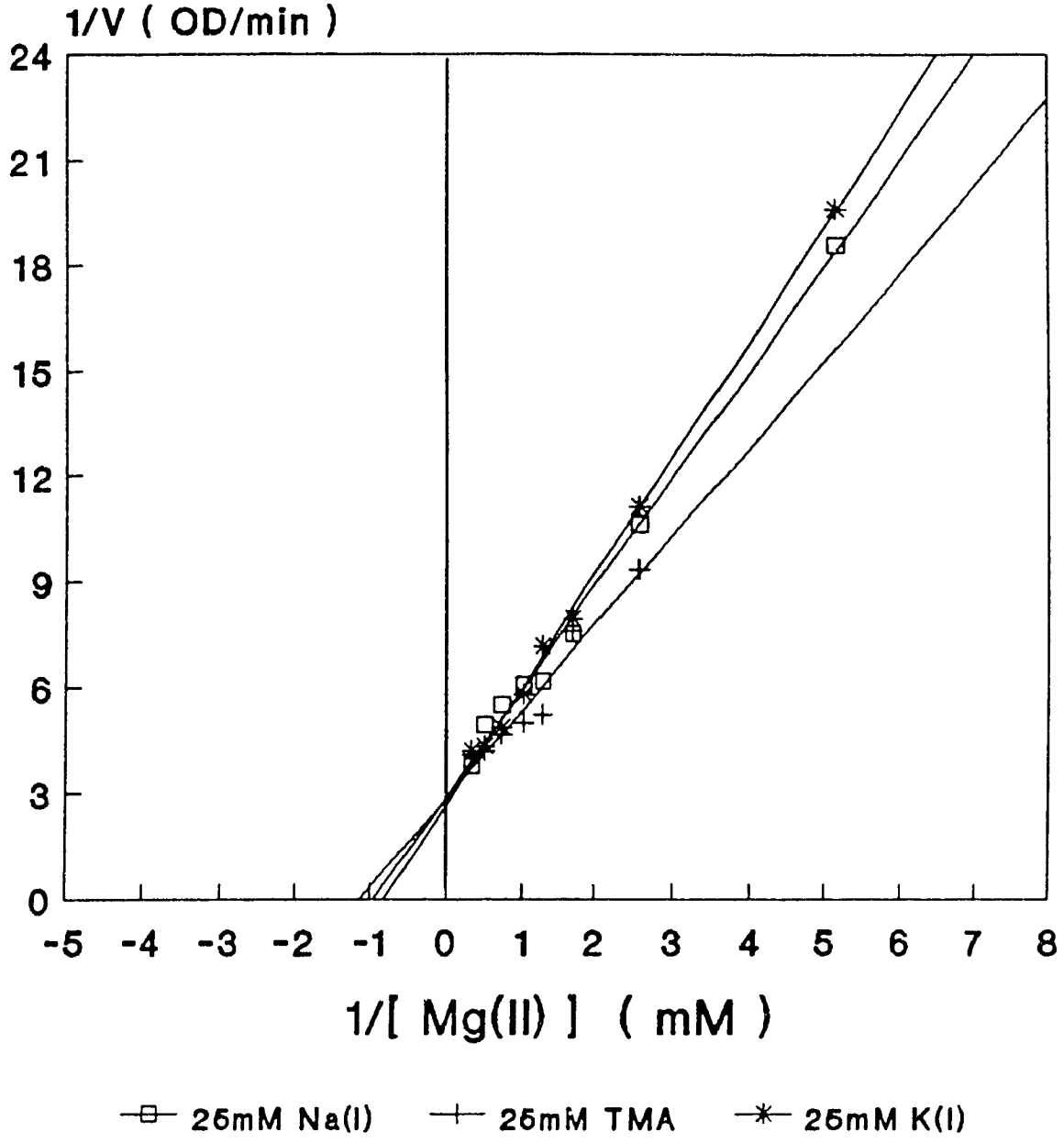

Enolase activity was measured as a function of [Mg(II)]

Figure 4.5 : Lineweaver - Burke Plot
Inhibition of Enolase Activity by Li(I)
pH 9.2 & 25mM Li

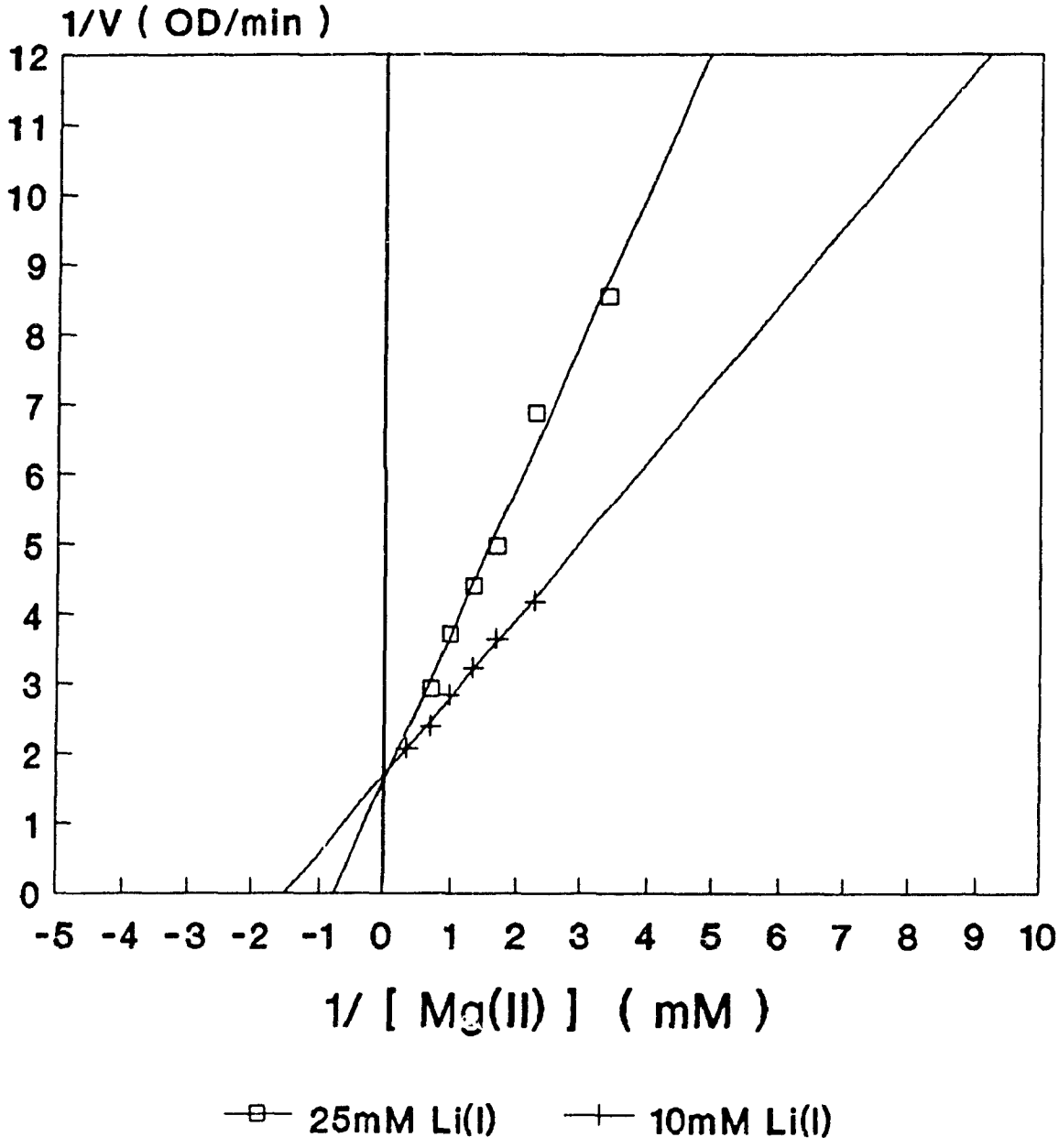

Enolase activity was measured as a function of [Mg(II)]

The effects of monovalent cations when the substrate is held constant and Mg^{2+} is varied are summarized in Tables 4.2 and 4.3. Figures 4.2 to 4.5 allow for a visual comparison. The results with Li^+, K^+ and Na^+ while slightly varied do appear to most closely resemble simple competitive inhibition with a common intersection at V_{max}. This would imply that Li^+ (as well as the other monovalent cations) binds to a different site on the enzyme at pH 7.1 than at pH 9.2.

There is though, a less dramatic rationale or explanation which may account for this difference in the observed inhibition patterns

4.4 : Type of Inhibition

From the Lineweaver-Burke plots at pH 9.2 , when PGA is held constant and Mg^{2+} is varied, Li^+ appears to be a competitive inhibitor. How can we account for this apparent change in inhibition from hyperbolic mixed type to competitive as pH is raised from 7.1 to 9.2? It may be explained assuming that there has been no change in the enzyme-cation complexes that are formed and the step inhibited by Li^+ is now a fast step in the reaction and therefore no decrease in V_{max} is observed. In Scheme 1 (below), this is equivalent to β=1; the complex with both Mg^{2+} and Li^+ bound to the enzyme still forms but the enzyme has the same activity with and without Li^+ bound ("partial competitive inhibition"). In the case of the other monovalent cations at pH 9.2, the step which is inhibited by Na^+ and K^+ must be fast as well and β is still 1.

The factor α is the factor by which K_s changes when the inhibitor occupies the enzyme. Both ES and ESI form product, but at different

rates. At any [I], the overall velocity at which product is formed is $k_p[ES] + \beta k_p[ESI]$, where $\beta<1$. From the equilibria we can see that an infinitely high substrate concentration will not drive all the enzyme to the ES form. At any given inhibitor concentration, a portion of the enzyme will exist as the less productive ESI form. Consequently, V_{max} will decrease in the presence of the partial noncompetitive inhibitor.

Scheme 1 :

Inhibition may be expressed by this general expression :

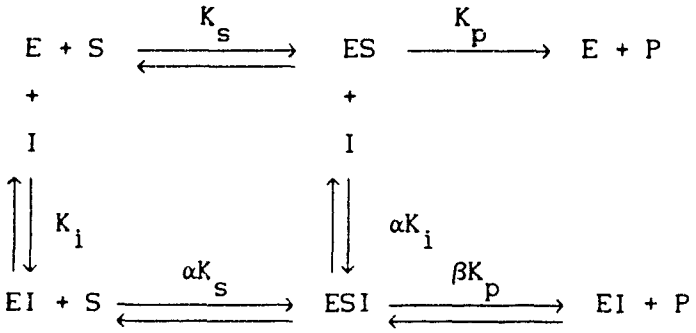

$1<\alpha<\infty$ & $0<\beta<1$; partial mixed-type inhibition
$1<\alpha<\infty$ & $\beta=1$; partial competitive inhibition
(Segal, 1975)

Partial competitive inhibition cannot be distinguished from pure competitive inhibition simply by plotting V versus [S] in the presence and absence of inhibitor or by the corresponding reciprocal plots (Segal, 1975). It is possible to distinguish the two by plotting V versus [I] at a fixed [S], as in Figure 4.6. In pure competitive inhibition, velocity can be driven to zero. From the equilibria describing partial competitive inhibition, we can see that at a fixed [S], an infinitly high [I] will drive all the enzyme to the EI and ESI forms. Since the ESI form can produce product the velocity can never be

Figure 4.6 : Vary [I] at Constant [S] at pH 9.2 & 1mM Substrate

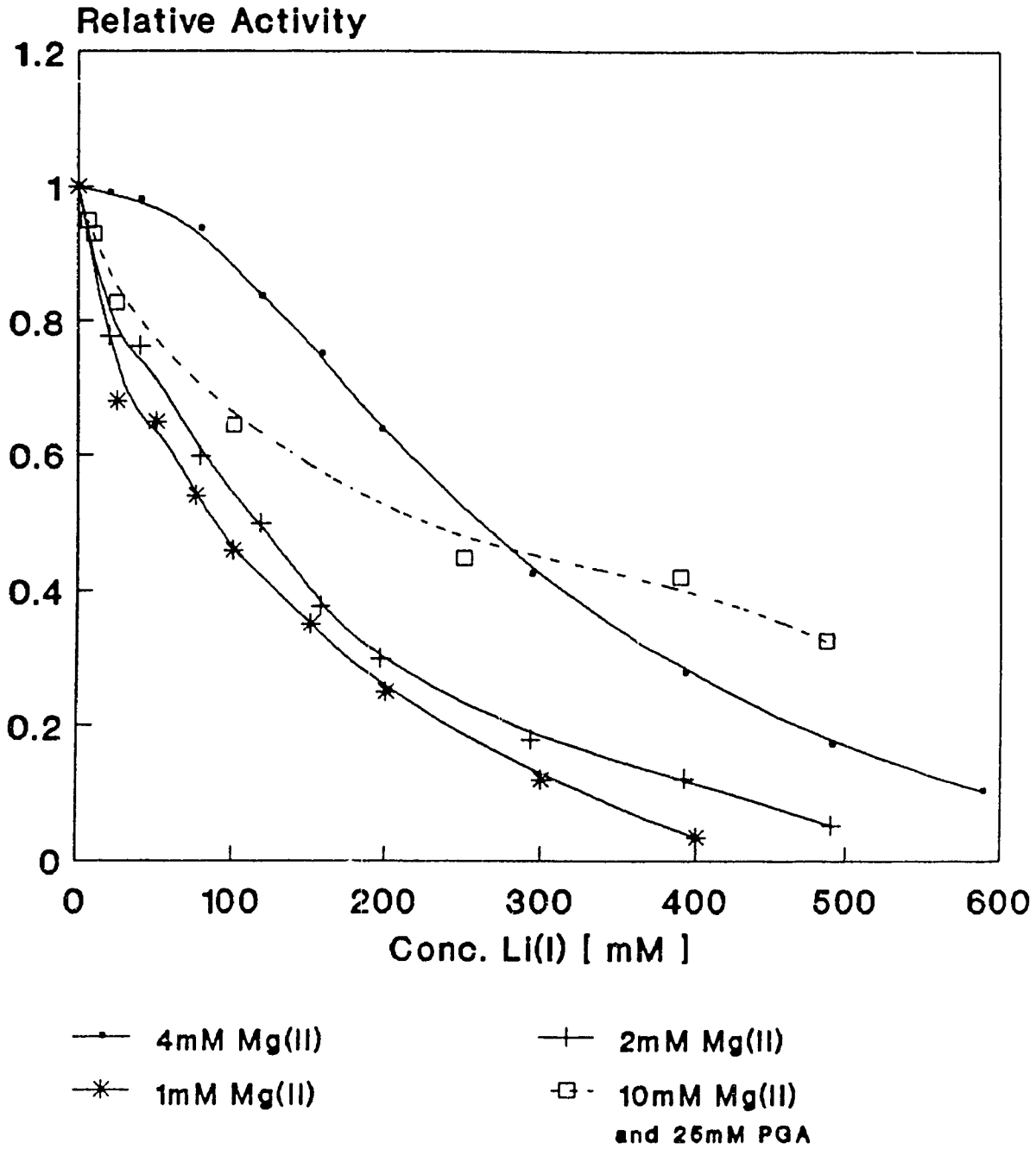

driven to zero.

Because of the effects of high ionic strength on the enolase reaction, Figure 4.6 is not necessarily open to a straight forward evaluation. Keeping that in mind, a case can be made for the velocity approaching a limiting value greater than zero.

Additionally, there may be another possible (plausible?) explanation to account for the change in the pattern of inhibition for monovalent cations when going from pH 7.1 to pH 9.2 without having to invoke a change in binding sites.

To do this, one must ask how does the analysis of Fig. 4.6 (or Scheme 1) take into account the effects of [I] on α ? If $\alpha >> 1$ the reaction approaches pure competitive inhibition. In this case the [EI] complex has very little affinity for [S] and the [ES] complex has very little affinity for [I]. Clearly, Li^+ increases the K_m for Mg^{2+}. Therefore it may be argued that at pH 7.1 $\alpha > 1$ but is not so great that binding (ESI form) does not occur. However, at pH 9.2 α is large enough that the reaction becomes pure competitive. This hypothesis does not require any change in binding sites. Simple steady-state kinetics will not resolve this question.

Even though we have not unambiguously distinguished if Li^+ inhibition at pH 9.2 is partial competitive inhibition, it is consistent with all the other data in that the change from "partial non-competitive" to "partial competive" due to a change in the rate limiting step(s) is a plausible simple explanation. It is a much more likely explanation than Li^+(or the other monovalent cations) competing

with Mg^{2+} for its binding site.

4.5: Binding of Divalent Metals to Apoenolase

In order to properly perform NMR experiments to probe the mechanism of inhibition, on enzyme activated by Ni^{2+} and "non-activated" by Ca^{2+} it was necessary to at least outline some basic kinetic parameters. Certain divalent cations can inhibit yeast enolase by binding at sites that are distinct from those metal binding sites normally associated with catalytic activity. By using a buffer that did not compete with metal ions (tetrapropylammonium borate) Zn^{2+}, Co^{2+}, Mn^{2+}, Cd^{2+},and Ni^{2+} were found to exhibit similar inhibitory characteristics (Elliot and Brewer, 1980). Inhibition by these metals is alleviated by the addition of imidazole or tris buffer. While imidazole will bind to divalent metals it is not universally accepted that tris binds divalent metals. Data from Calbiochem (taken from Buffers: A Guide for the Preparation and use of buffers in biological Systems) suggests negligible binding of Mn^{2+}, Mg^{2+}, Ca^{2+} and Cu^{2+} to Tris. However, Tris buffer was not chosen for these current experiments due to its interference on the NMR spectra of PGA.

The inhibition of enolase by a metal ion could result from a number of events. The inhibitory metal could occupy the conformational site and disrupt either substrate binding or a subsequent step in catalysis. The inhibitory metal could bind at the catalytic metal binding site in such a way that further reaction is reduced. At very high concentrations of metal ion, chelation of the substrate away from the

active site of the enzyme may occur (Bell, 1977). Finally an inhibitory site might exist which is independent of the sites for catalytic and conformational metals, and for substrate. The inhibition could then result from either direct interaction with the catalytic process or from conformational changes induced in the enzyme which bring about the inhibition. (Elliot and Brewer, 1980).

Figure 4.7 (see also Table 4.4) graphically portrays the inhibition of yeast apoenolase due to Ni^{2+}. The plot clearly shows competitive inhibition, with Ni^{2+} competing with Mg^{2+} for the same binding sites. Thus we may feel confident that activity we will be monitoring is not being affected by artifactual binding of Ni^{2+} to nonproductive sites on the enzyme.

The K_m for Ni^{2+} under the conditions employed for NMR determinations (5mM PGA, pH 7.1) is 0.047mM ± .009mM . To give a perspective on the relative binding strength and low activity exhibited by Ni^{2+}, the other divalent metals which had been previously screened for activity are included in Table 4.5.

Figure 4.7 : Lineweaver - Burke Plot Inhibition of Enolase Activity by Ni(II) pH 7.1 & 5mM PGA

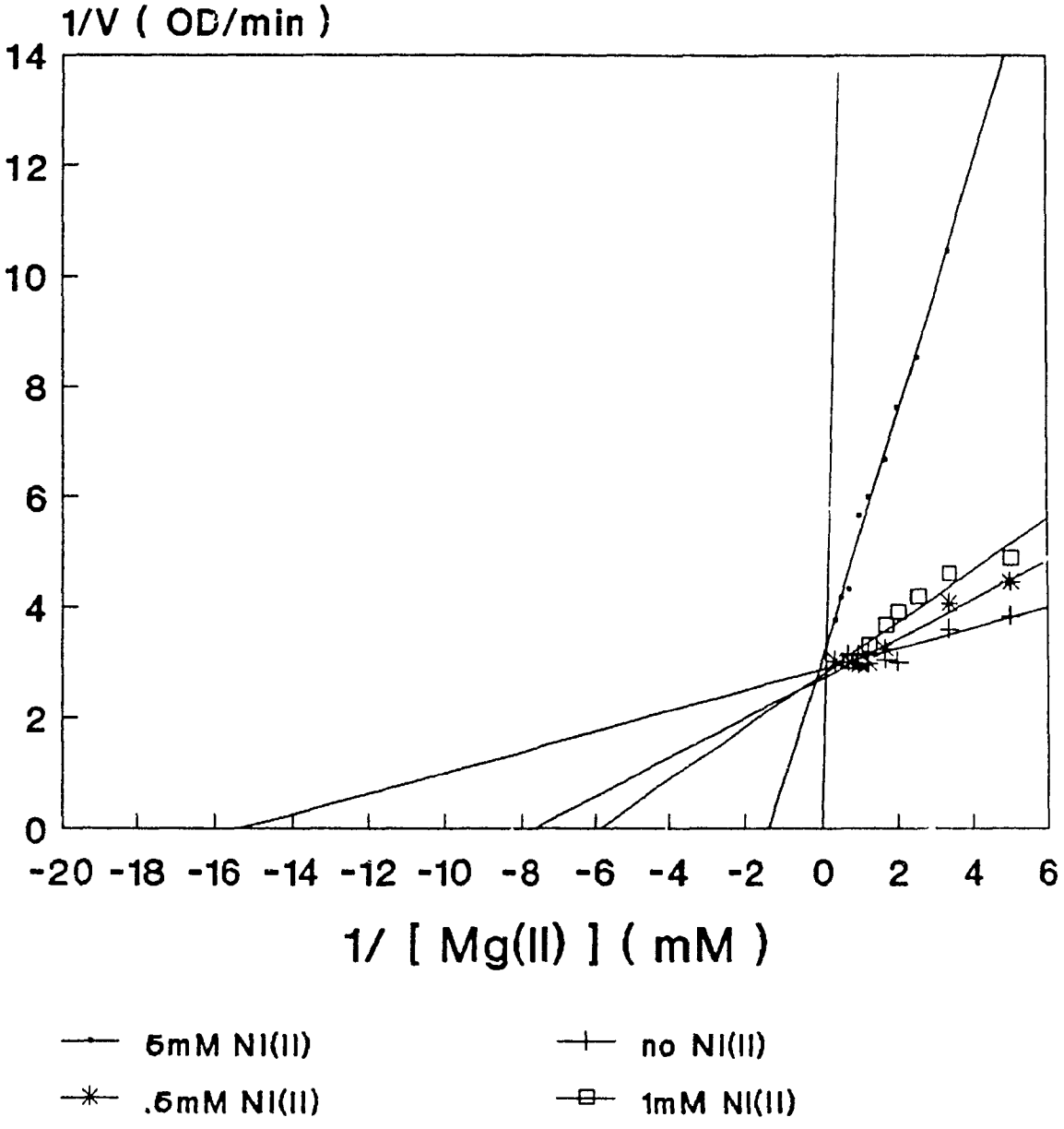

Enolase activity was measured as a function of [Mg(II)]

Table 4.4 : Effects of Ni^{2+} on Kinetic Parameters of Enolase at pH 7.1 and 5mM PGA

Ni^{2+} conc. (mM)	K_M Mg^{2+} (mM)	V_{Max} (relative)
0.0	.059 ± .019	1.000 ± 3.76%
.5	.118 ± .024	1.046 ± 3.32%
1.0	.211 ± .042	1.073 ± 5.50%
5 0	.774 ± .072	0.973 ± 3.87%

Table 4.5 : Effects of Various Divalent Cations on the Kinetic Parameters of Apoenolase at pH 7.1 and 5mM PGA

metal ion	K_m (mM) for metal ion	V_{max} (relative)*
Mn^{2+}	.098 ± .021	.158 ± 11.39%
Cd^{2+}	.760 ± .048	.020 ± 3.00%
Ni^{2+}	.047 ± .009	.026 ± 0.43%
Zn^{2+}	.812 ± .117	.105 ± 8.47%
Ca^{2+}	no activation	no activation

* relative to V_{max} with Mg^{2+} at pH 7.1 and 5mM PGA

both (Shen and Westhead, 1973). By using NMR to monitor solvent exchange with the hydrogen on carbon 2 of PGA we can ascertain this information regarding inhibition by Ni^{2+}. If the steps subsequent to proton abstraction are inhibited such that they are now rate limiting, then a significant rate of exchange should occur. In this way inhibition by Ni^{2+} at pH 7.1 may mimic or resemble inhibition at pH 9.2. If this is the case, no primary kinetic isotope effect ($V_{max(H)}/V_{max(D)}$) should be present. If Ni^{2+} does not act on the steps following proton abstraction or if it further inhibits proton abstraction , no significant exchange will occur.

In this same way we can look at inhibition by the nonactivator Ca^{2+}. If the lack of activity is due to a total retardation of the reaction steps following proton abstraction then significant exchange will be observed. If Ca^{2+} inhibits proton abstraction or if the metal does not allow for this first step in the proposed reaction mechanisn to take place, then no exchange between the carbon-2 hydrogen of PGA and solvent will take place

Chapter 5 Use of NMR as a Probe of Enolase Reaction Mechanism

5.1: Introduction

Proton NMR was used to follow the exchange of solvent deuterium (D_2O) with the carbon-2 hydrogen of PGA. Figures 5.1 and 5.2 reveal typical spectra for PGA and PEP produced, respectively, on the Bruker WP 80SY. According to Shen and Westhead (1973) the C-2 hydrogen of PGA is split by the phosphorus and other protons to give a cluster of seven peaks. As can be seen in Fig. 5.1 the septet of the C-2 hydrogen is clearly visible at the edge of the solvent peak. All seven peaks are discretely separated and the most prominent peak , located in the middle of the septet, is centered at 4.49 ppm. The protons of carbon-3 are visible as a broad, poorly resolved quartet. The location of the highest signal in this quartet is 3.91 ppm. The use of a higher field instrument (ie: 500MHz) would undoubtedly give greater resolution and separation between the peaks of the carbon-3 protons but for the purposes of the present experiments (quantifying one peak height with concentration of substrate), such refinement was unnecessary.

To positively ensure that the septet centered at 4.49 ppm is truly due to the carbon-2 hydrogen of PGA, a COSY pulse sequence experiment was performed. Chemical shift correlation via *J* coupling is a very useful technique for the interpretation of complex NMR spectra, particularly proton spectra, as it furnishes virtually automatic assignments of resonances. In this particular case COSY was used for a trivial assignment. The basic COSY pulse sequence is simply:

$\pi/2 - \tau - \pi/2$ - acquire, where τ is an incremented delay.

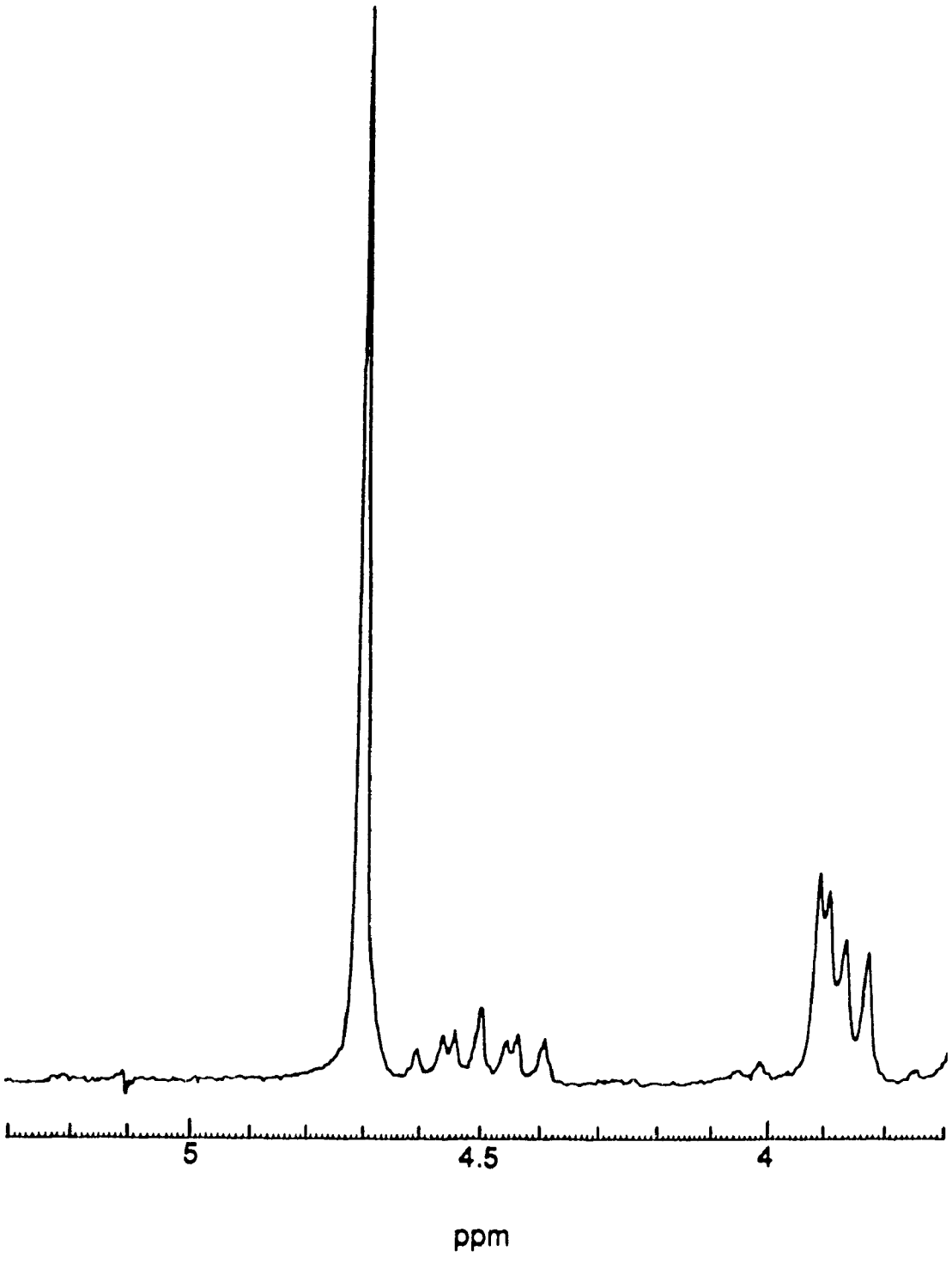

Figure 5.1: Proton NMR Spectrum of PGA at 80MHz

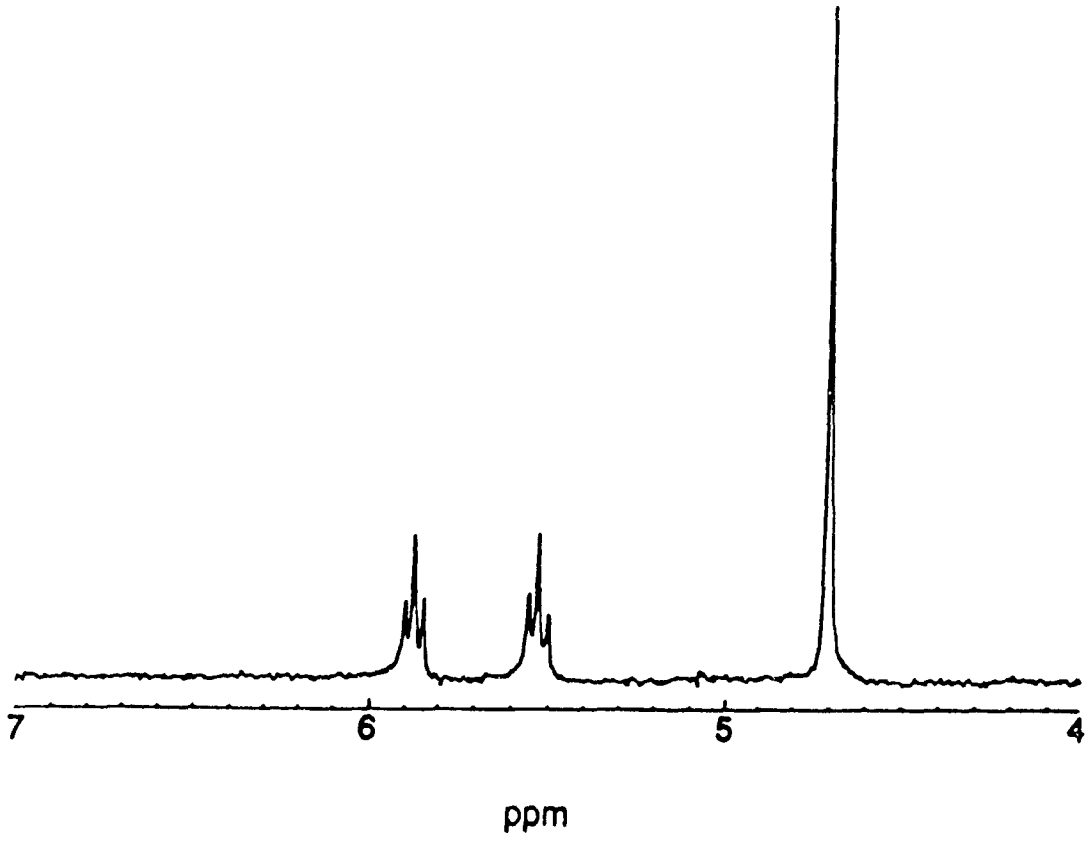

Figure 5.2: Proton NMR Spectrum of PEP at 80MHz

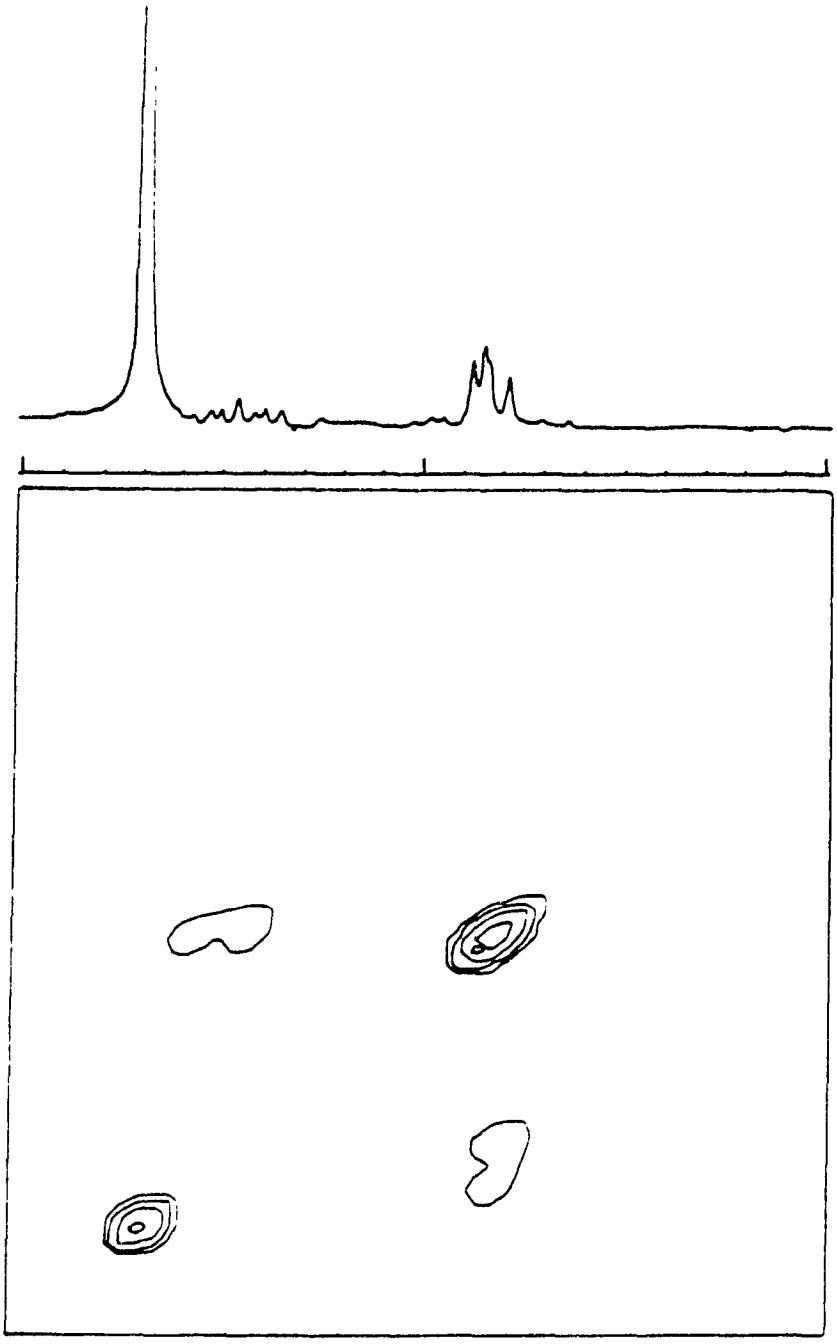

Figure 5.3: ^{1}H COSY of PGA

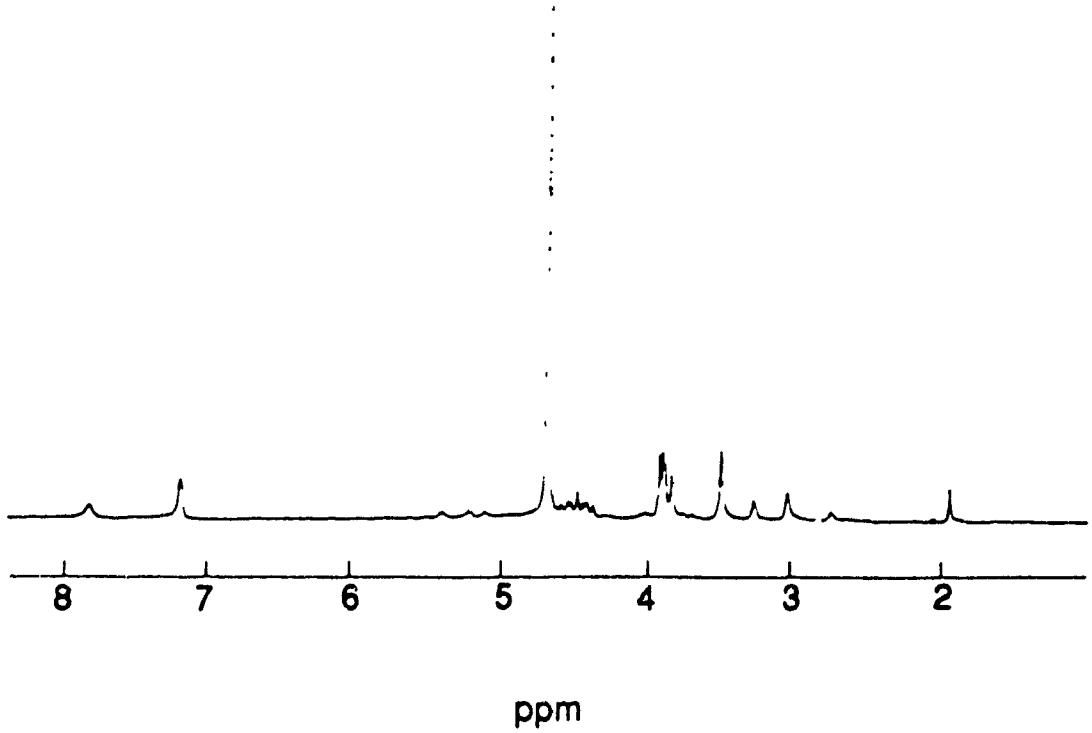

Figure 5.4: Proton NMR Spectrum of PGA, EDTA, Imidazole and Mg acetate ("Reaction media")

In the COSY experiment, the spins (in a simple vector diagram) precess under the influence of both the chemical shift and the *J* coupling. It is the precession under the latter influence that gives rise to the "cross peaks". The off-diagonal "cross peaks" tell us which chemical shifts are connected to which (Sanders and Hunter, 1987). From Figure 5.3 it is readily apparent that the resonances of the septet are related to the quartet.

The proton NMR signals due to the other constituents of the reaction media used (EDTA, Mg acetate and imidazole) did not interfere or mask the peaks due to PGA and were readily identified by the literature values for their chemical shifts (Bovey, 1988). Figure 5.4 gives a typical spectrum of the complete reaction "mix".

5.2: Exchange Rate at pH 7.1 and 9.2

Shen and Westhead (1973) have reported that, as the pH increases from 6.5 to 9.0, the kinetic isotope effect decreases to 1.0, indicating that there has been a change in the rate-limiting step(s) of the reaction, with proton abstraction no longer being a slow step. At pH 7.1, proton abstraction is partially rate-limiting and the kinetic isotope effect is greater than one (Kornblatt and Musil, 1990; Dinovo and Boyer, 1971).

Figure 5.5 shows a very slow rate of exchange at pH 7.1 where the isotope effect is strong. This agrees with the picture of nearly rate-limiting proton abstraction. At pH 9.2, where there is almost no primary isotope effect a moderate rate of exchange is expected Initially, this was not observed. This proved to be due to the lack of

Figure 5.5 : Exchange at pH 7.1
25mM PGA and 10mM [Mg(II)]

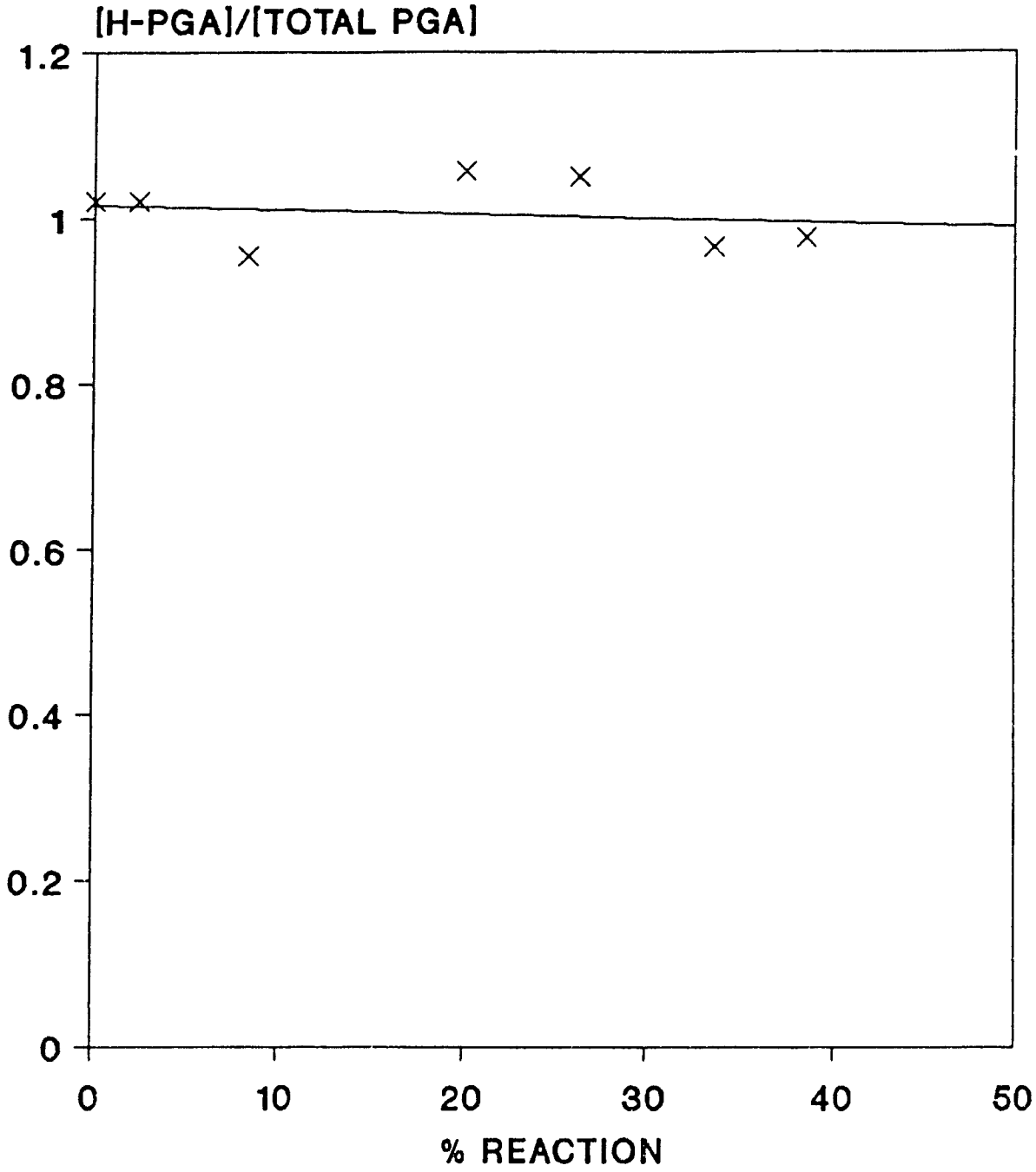

saturating Mg^{+2} at the concentration of substrate used for the proton NMR experiments: 25mM PGA. Initial experiments were performed at 1mM Mg acetate. From Figure 5.6 it can be seen that no appreciable exchange takes place at this concentration of activating metal. Upon an increase to 10mM Mg^{+2} a moderate rate of exchange can be measured (≈ 50% exchange in remaining PGA after 50% conversion). An examination of Shen and Westhead's (1973) protocol reveals that they too needed to use a saturating level of Mg^{+2} to measure an identical rate of exchange. If no exchange were found at pH 9.2, the results would show either sequestration of the removed proton by the enzyme or that catalysis proceeds by a carbonium ion mechanism in which slow hydroxyl ion removal precedes rapid proton removal and product release.

5.3: Exchange Rate with Monovalent Cations

The rate of exchange of the hydrogen on carbon-2 of PGA with solvent was measured during the enzymatic reaction at pH 9.2 and the effects of Li^+ and Na^+ on this exchange were determined. The results are shown in Figure 5.7. Significant exchange occurs at pH 9.2; this exchange is not affected by the presence of either 10mM Li^+ or 25mM Na^+. The use of 25mM TMA^+ as a control (Figure 5.8) also did not affect the rate of exchange. TMA^+ has been used as a control because of its large size in comparison to Li^+ and/or Na^+. It is not expected that TMA^+ would bind to a site specific for either Na^+ or Li^+ due to this size differential and thus any effects caused by TMA^+ are solely attributable to ionic strength effects.

According to the reaction mechanism shown in Figure 1.2, exchange of

Figure 5.6 : Exchange at pH 9.2
as a Function of [Mg(II)]

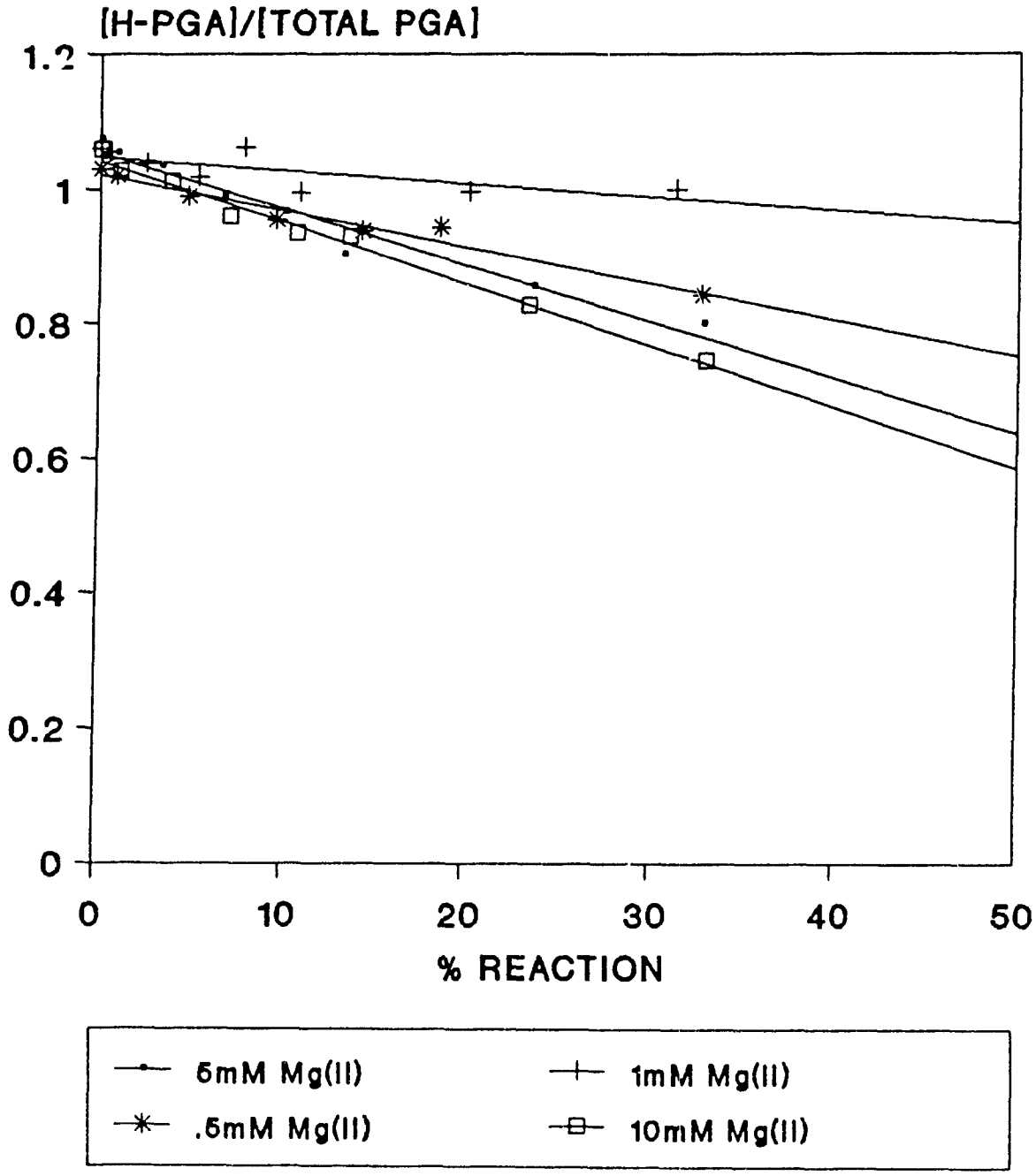

Figure 5.7 : **Exchange at pH 9.2**
Effects of Li(I) and Cl(I)

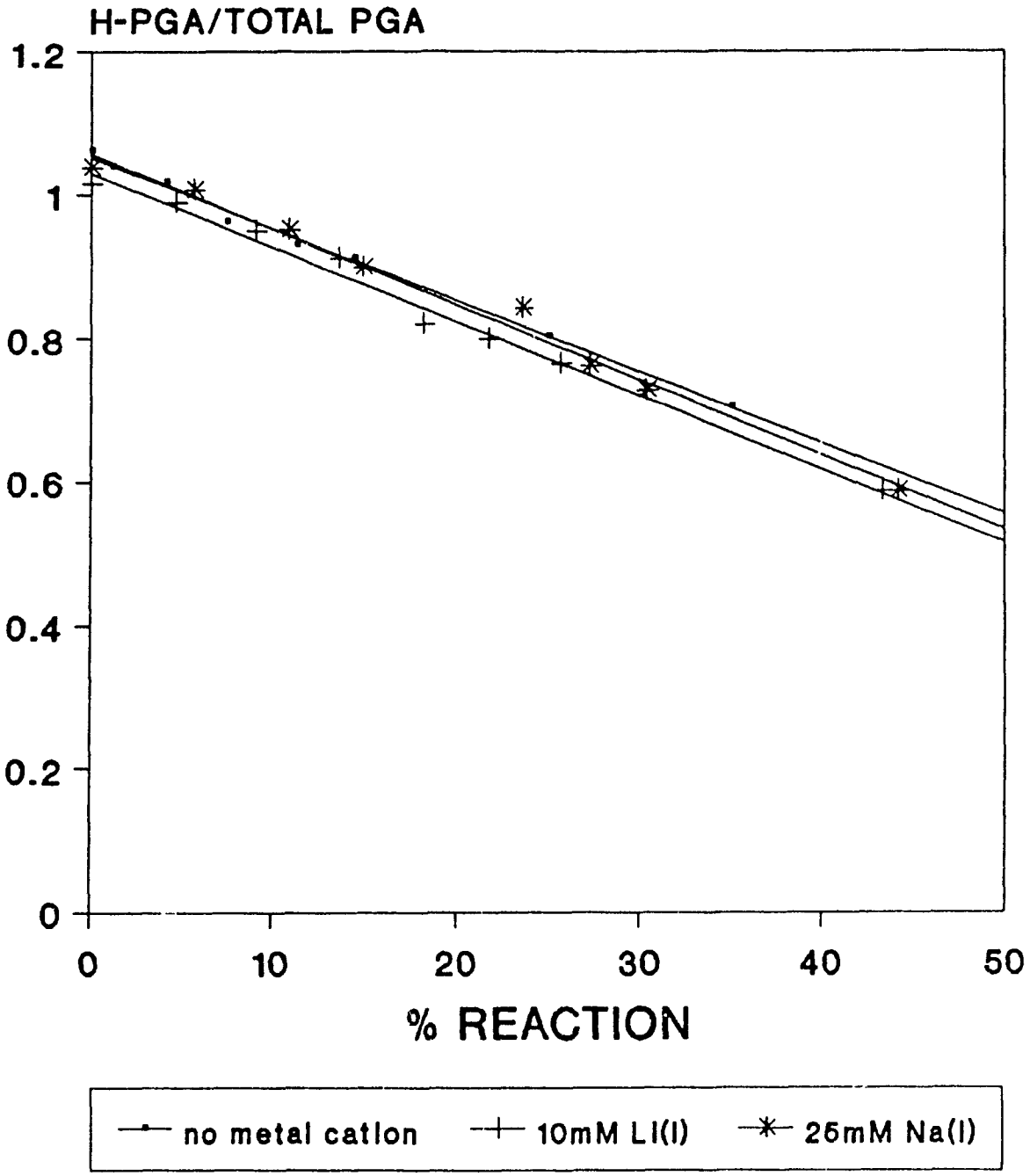

Figure 5.8 : **Exchange at pH 9.2**
25mM PGA

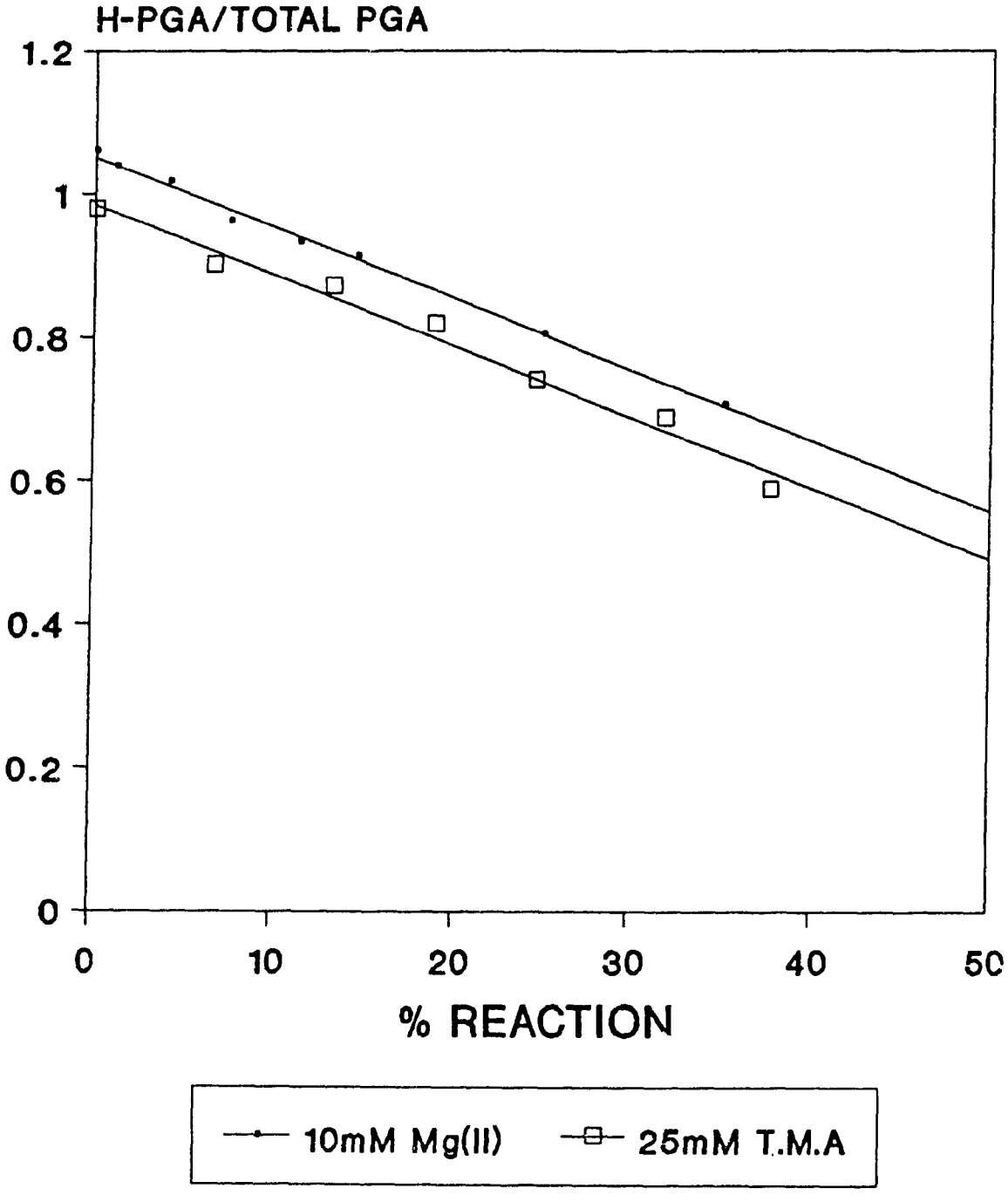

the hydrogen on C-2 of PGA with solvent can occur by a reversal of steps prior to product release. The extent of hydrogen exchange will be determined by the partitioning of the carbanion between product (PEP) formation and reprotonation to form PGA. At pH 7.1, where proton abstraction is a slow step in the mechanism no exchange is observed. At pH 9.2, where proton abstraction is fast and is followed by one or more slower steps, exchange is observed. The presence of Li^+ has no effect on the exchange, and therefore does not decrease the rate of proton abstraction. These results also suggest that the step inhibited by Li^+ (and Na^+) is product release (PEP and/or Mg^{2+}) since inhibition of hydroxyl ion removal, which immediately follows proton abstraction, would be expected to increase the rate of exchange.

5.4: Exchange Rate for Apoenolase Activated by Ni^{2+} and Ca^{2+}

According to the results of Stubbe and Abeles (1980) the rate of proton abstraction from carbon-2 of PGA, catalyzed by Mn^{2+}-enolase, increases while the rate of dehydration of PGA decreases. This is all in relation to the reaction catalyzed by Mg^{2+} activated enolase. Therefore it was of interest to see if this might also be true for other metals - especially poor activators or non-activators. Does proton abstraction remain efficient and are later steps in the reaction pathway blocked?

Figure 5.9 shows the result of the exchange experiment performed with apoenolase activated by Ni^{2+} at pH 7.1. Unexpectedly, no significant rate of exchange between solvent and the hydrogen on

Figure 5.9 : Exchange at pH 7.1
Apoenolase activated by Ni(II)

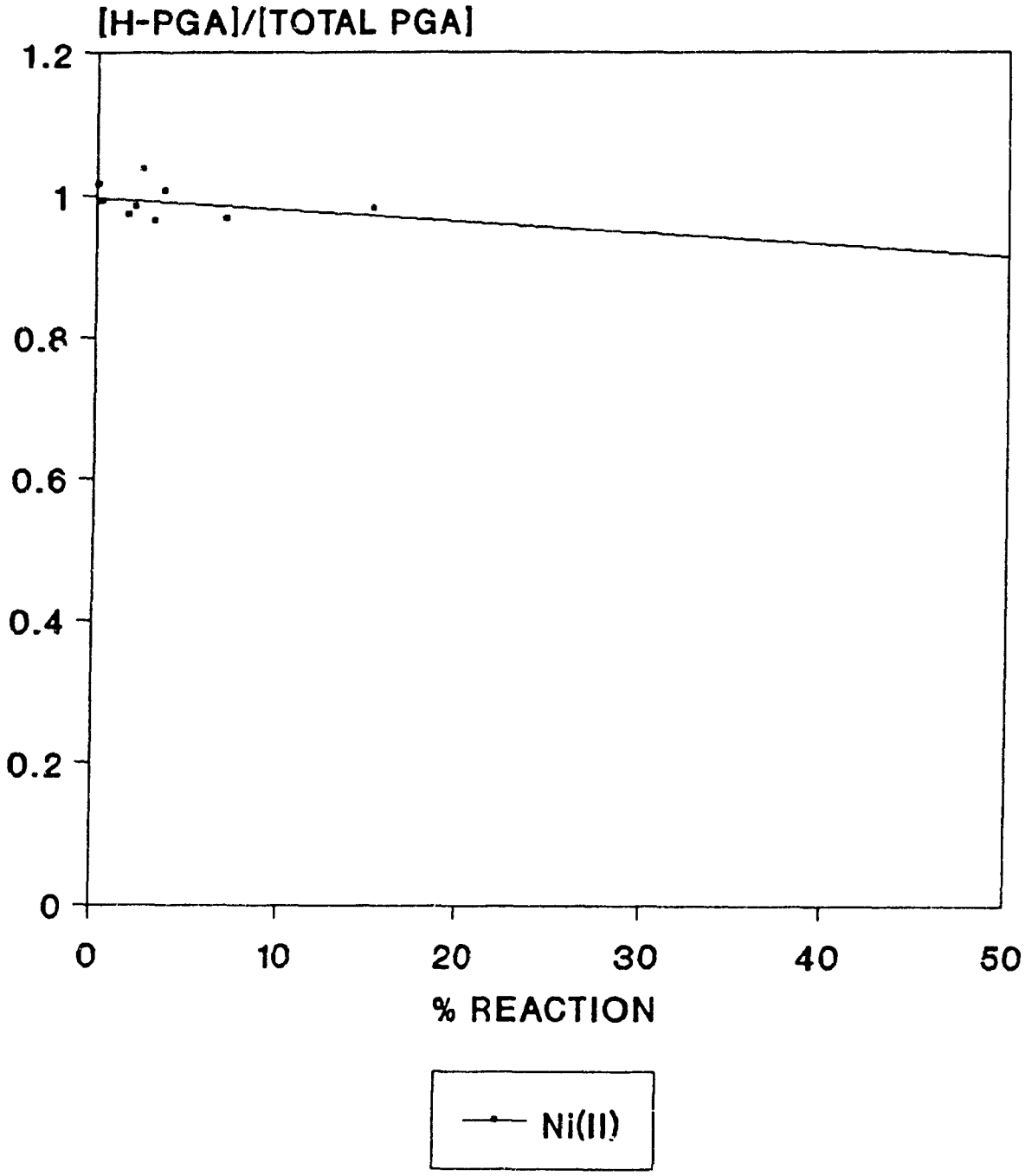

carbon-2 of PGA could be observed. This implies that proton abstraction is still partially rate-limiting and that all subsequent steps are fast in comparison. Less effective metals have been seen to decrease the efficiency of steps following proton abstraction (Shen and Westhead, 1973). Their inhibition has been likened to that seen at alkaline pH.

If a rate of exchange could be detected then differentiation between inhibition of hydroxyl ion removal or product release could be achieved by ^{18}O exchange studies. Increases in ^{18}O incorporation would implicate inhibition of product release whereas no change in the exchange rate would imply that hydroxyl ion removal has been slowed.

Binding of Ca^{2+} does not produce activity in enolase Catalysis has been found to proceed only if the conformational metal ion can can favor an octahedral co-ordination geometry (Brewer, 1985). Magnesium is more similar in its chemical properties to zinc and cadmium than to calcium, and these three activating metals share a tendency to form bonds of a more covalent character (Brewer and Collins, 1980).

The rate of solvent exchange with the carbon-2 hydrogen of PGA, for apoenolase bound to the non-activator Ca^{2+} at pH 7 1, was plotted against time (Figure 5.10). No rate of exchange was observed. Clearly, Ca^{2+} does not inhibit the steps following proton abstraction. In fact we may conclude that with Ca^{2+} bound enolase not even the first step in the reaction pathway - proton abstraction - occurs. Since no PEP is formed, if proton abstraction was to occur then one of the later steps must be totally inhibited and a measurable exchange should have been observed. Brewer (1985) had previously speculated that it was uncertain

Figure 5.10 : Exchange at pH 7.1
Apoenolase activated by Ca(II)

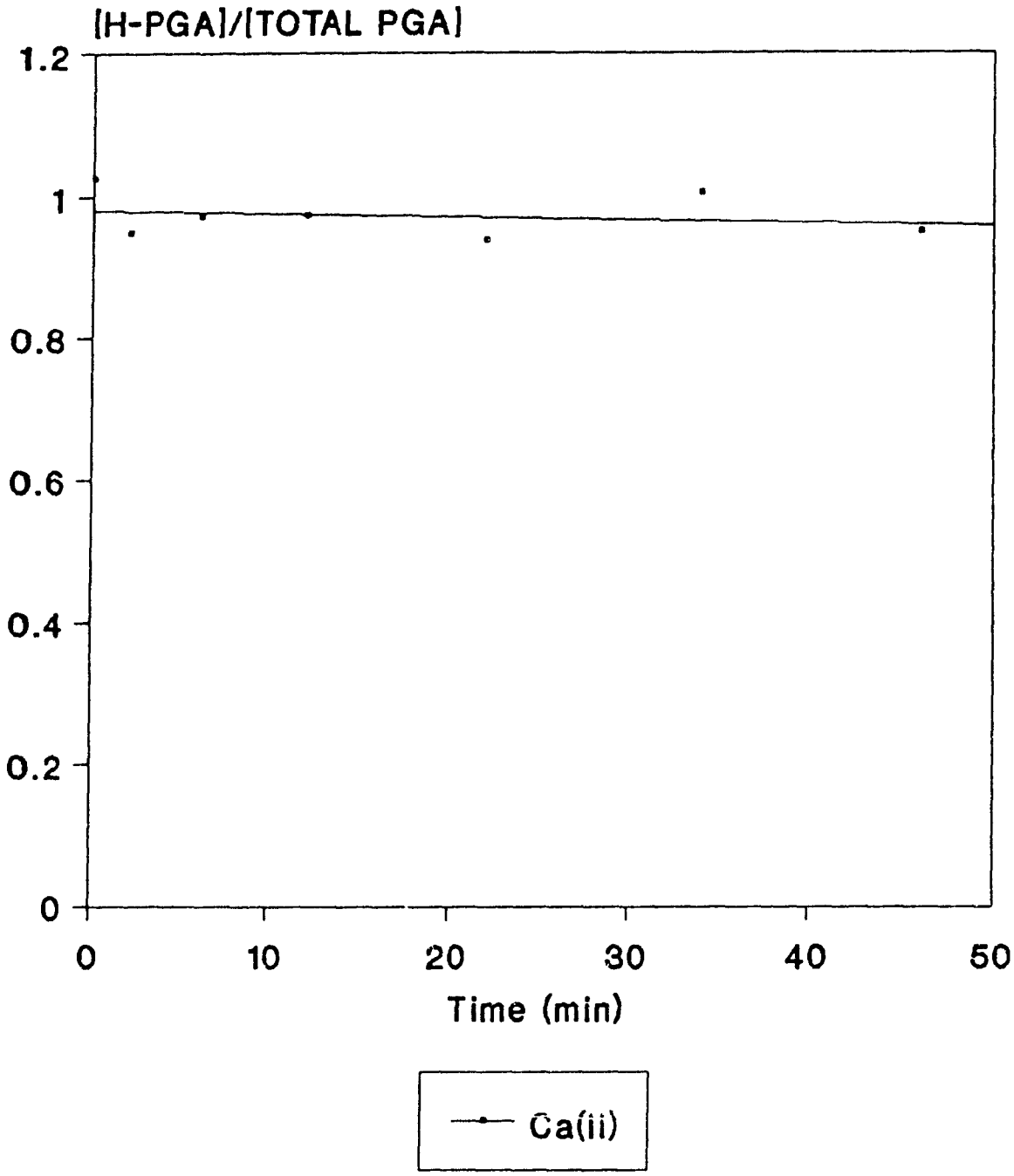

whether the non-activated enzyme is capable of proton abstraction.

5.5 Kinetic Isotope Effects under Experimental Conditions

All of the previous analyses are contingent on the fact that the binding of Li^+ decreases the activity of the enzyme; that is, the enzyme-Li^+ complex is active. In order to verify whether a specific step in the reaction has been slowed or not, the kinetic isotope effect on V_{max} in the presence and absence of Li^+ was measured. At pH 7.1, proton abstraction is partially rate limiting and the kinetic isotope effect is greater than 1.0 (Shen and Westhead, 1973). If Li^+ inhibited either proton abstraction or another partially rate limiting step, one would expect to see a change in the kinetic isotope effect.

It has been previously shown (Kornblatt and Musil, 1990) that Li^+ does change the value of $V_{max(H)}/V_{max(D)}$ supporting the conclusion that the enzyme with Li^+ bound is active. At pH 7.1 as $[Li^+]$ increases, the kinetic isotope effect on V_{max} decreases. Li^+, therefore, cannot be decreasing the rate of proton abstraction relative to the rates of the other steps in the reaction but must, instead, be decreasing the rate of another step that is also partially rate limiting

Table 5.1 lists the measured kinetic isotope effects on V_{max} at pH 9.2. In agreement with Shen and Westhead (1973) it may be seen that at pH 9.2 the kinetic isotope has decreased to $\simeq$ 1.09 indicating that there has been a change in the rate limiting step(s) of the reaction, with proton abstraction no longer a slow step. This also serves to verify the results obtained measuring solvent exchange through NMR. The addition of 10mM Li^+ has basically no effect on the value of

$V_{max(H)}/V_{max(D)}$ and thus must be decreasing the rate of a step other than proton abstraction.

With Ni^{2+} activated apoenolase no significant exchange rate between the hydrogen of C-2 of PGA with solvent was measured during the enzymatic reaction at pH 7.1. This would indicate that proton abstraction remains a slow step in the reaction. The kinetic isotope effect on V_{max} should then be greater than one, and was determined to be 1.8 (fig. 5.11). This is comparable to the kinetic isotope effect for enolase activated by Mg^{2+} at pH 7.1 (Shen and Westhead, 1973 ; Kornblatt and Musil, 1990).

TABLE 5.1 : Kinetic Isotope Effects at pH 9.2

[M^+]	$V_{max(H)}/V_{max(D)}$
0	1.09 ± .12
10mM Li^+	1.03 ± .07

A kinetic isotope effect is also observed on K_M for Mg^{2+} as well as for Ni^{2+}, indicating that $K_m \neq K_s$. The effect of Li^+ on the K_M for Mg^{2+} and of Ni on enolase activity may include both an effect on binding (K_s) and an effect on one or more of the other rate constants that contribute to K_m.

From the observed kinetic isotope effect and solvent exchange data we can conclude that for yeast enolase activated by Ni^{2+}, proton abstraction is still partially rate limiting and that the decreased

Figure 5.11 : Kinetic Isotope Effect
For Ni(II) Activated Apoenolase; pH 7.1

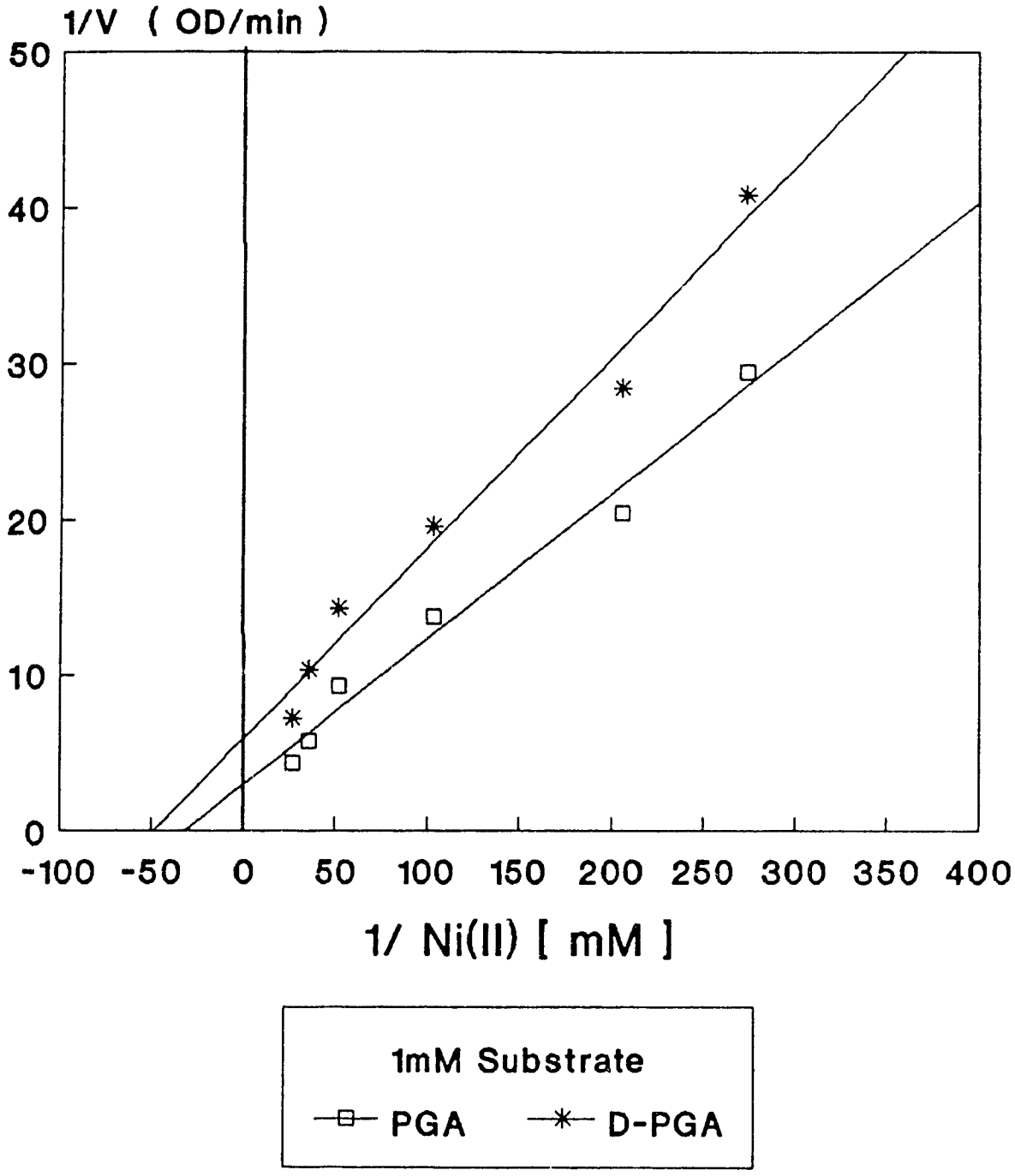

rate of reaction for enolase activated by Ni^{2+} is not solely due to the inhibition of either hydroxyl ion removal or product release. Shen and Westhead's (1973) kinetic studies on the effect of substitution of deuterium for hydrogen at carbon-2 of PGA are not consistent with this finding. Using Co^{2+} as activating metal, which gives approximately the same relative maximum rate as Ni^{2+} (Brewer, 1981), no isotope effect over a pH range of 6.5 to 8.0 was obtained. Activation of enolase by Co^{2+} appears to mimic the effects of activation at alkaline pH's; hydroxyl ion removal or possibly product release is rate limiting. Is this a general phenomena for all less effective metals? The kinetic isotope effect for Mn^{2+} activation of 1.5 (Shen and Westhead, 1973) agrees very closely to that found for Ni^{2+}.

The inconsistency in isotope effect, and hence mode of inhibition, between Co^{2+} and Ni^{2+}, two apparantly similar activators may be reconciled by an evaluation of the results of Brewer and Collins (1980). They looked at the interaction of the competitive inhibitor AEP with apoenolase and various metals. AEP has the useful property of changing in absorbance upon binding to enolase in the presence of activating metals This is an all or none reaction: metals that do not produce enzymatic activity do not produce the absorbance change in AEP whereas metals that permit any level of enzymatic activity produce the same change. The aldehyde analogue of the substrate, TSP, behaves similarly. Because of their much tighter binding to the enzyme than the natural substrate or product (PGA or PEP), they have been suggested as "transition state analogues".

Titrations of apoenolase-TSP solutions were carried out using a number of metals. The rate of absorbance change in TSP is the same whether nickel or magnesium is present. When zinc and cadmium are used as activators, the rate of absorbance change (with AEP in this case) is slowed but eventually the full absorbance change is produced. The reaction produced by magnesium is also slower as pH is increased. It may be possible that the pH affects the rate of absorbance change by the same mechanism as that of the less effective activating metals. The rate limiting step in the normal enzymatic reaction is proton removal from carbon-2. However, some step connected with the metal can be limiting. This inhibition appears similar to that seen at high pH and at more alkaline pH where the step inhibited is is either hydroxyl ion removal or product release

From the kinetic isotope data as well as the AEP binding data the less effective metals are clearly seen to decrease the efficiency of either hydroxyl ion removal or product release or both. Using the AEP binding criteria, nickel does not appear to behave like other poorly activating metals but rather like Mg^{2+}. The same is true for the hydrogen exchange data and kinetic isotope effect on V_{max} for Ni^{2+} activated apoenolase. In each case nickel gives anomalous results as compared with the other "poor" metals and proton abstraction continues to dominate the reaction rate. It is proposed that the inhibition produced by nickel activation is unique and unlike that of the other less effective activators.

Chapter 6 Preliminary Findings on the Use of ^{13}C NMR for Detection of ^{18}O Exchange

6.1: Introduction

There are numerous examples of the effects of isotopic substitution upon the NMR resonance positions of various nuclei. ^{18}O isotope effects have been reported for ^{55}Mn and ^{95}Mo NMR spectra and for ^{31}P NMR spectra (Risely & Van Etten, 1979). Jameson (1977) had predicted an ^{18}O isotope effect on ^{13}C NMR spectra, in particular an upfield shift in ^{18}O labelled $^{13}CO_2$ which is dependent on the number of ^{18}O atoms in the molecule.

Risely & Van Etten (1979) observed such an isotope shift in ^{13}C NMR spectra and demonstrated its usefulness for studying oxygen exchange kinetics. Their original study employed natural abundance spectra and a Fourier transform instrument operating at 20 MHz for ^{13}C, showing that instruments of high magnetic field strength are not necessary for kinetic studies providing that curve resolution or electronic integration are employed. The quantitative data obtained from the resolved spectra closely approximated those obtainable by peak height measurements. Thus, the greater separation available from higher field strength instruments permits ever more convenient quantitation solely through the use of peak heights.

A series of studies by Risely and Van Etten (1981), as well as others, have shown that the ^{18}O isotope effect in ^{13}C NMR is a general phenomenon. The magnitude of the isotope induced shift is determined principally by the structure of the carbon-oxygen functional group. The

isotope effect is governed to a smaller degree by the through bond electronic influences of the substituted groups conjugation, and hybridization of the carbon atom.

Isotope effects are additive (Risely & Van Etten, 1980). Very small solvent effects have thus far been detected only in alcohols and bulk steric effects do not affect the magnitude of the isotope effect. When different functional groups are compared, there is no apparent correlation between carbon-oxygen bond length and the magnitude of the isotope effect.

The technique offers several advantages over mass spectrometry for following oxygen exchange reactions, primarily with respect to the ease of analysis, accumulation of data, and continuity of assay. As a tool for further elucidation on the mechanism of Li^{+} inhibition on enzymatic activity, the monitoring of an ^{18}O induced chemical shift appears useful.

What do we expect to see if we carry out the conversion of PGA to PEP catalyzed by enolase in $H_2{}^{18}O$? If Li^{+} inhibits product release (PEP and/or Mg^{+2}) more ^{18}O will be incorporated into PGA. If hydroxyl ion removal is slowed there should be no change in the amount of ^{18}O accumulated into PGA.

6.2.: ^{13}C NMR Identification of Peaks

The initial ^{13}C experiment, conducted to obtain a survey spectrum is, as a rule, always recorded under proton broadband noise decoupling (double resonance). The purpose of the second irradiation frequency is to simultaneously remove all carbon - proton scalar couplings with a

two-fold benefit;

1) a two times increase in the S/N ratio

2) a simplification of what otherwise may be a very complex spectra.

The decoupled spectrum will provide the chemical shift and the carbon number of the molecule. Fig. 6.1 represents the broadband decoupled ^{13}C spectrum of the standard quenched reaction medium, including PGA, Mg acetate and EDTA in imidazole buffer. From the literature values for the chemical shifts of Mg acetate, EDTA and Imidazole (Bovey, 1988), the three carbons of PGA can be tentatively assigned to the peaks located at 178.4ppm, 78.0ppm and 65.4ppm.

Because it is necessary to know which signal represents the C_3 carbon bound to ^{18}O, it is imperative to make an unambiguous distinction between the three carbons of PGA. The use of specific pulse sequences allows for spectral editing on the basis of CH_n multiplicities. The polarization transfer method chosen for this spectral editing was DEPT. Distortionless enhancement by polarization transfer is a pulse sequence closely related to refocused-INEPT (Insensitive Nuclei Enhanced by Polarization Transfer). Unlike INEPT, DEPT cannot be analyzed by simple vector models; it depends on the generation and manipulation of multiple-quantum coherences (Sanders and Hunter, 1987).

The pulse sequence for DEPT is:

$$^{1}H \quad (\pi/2)_x - t_D - (\pi)_x - t_D - (\theta)_y$$

$$^{13}C \quad (\pi/2)_x - t_D - (\pi)_x - t_D - \text{Acquire}$$

where $(\theta)_y$ is a pulse of variable flip angle

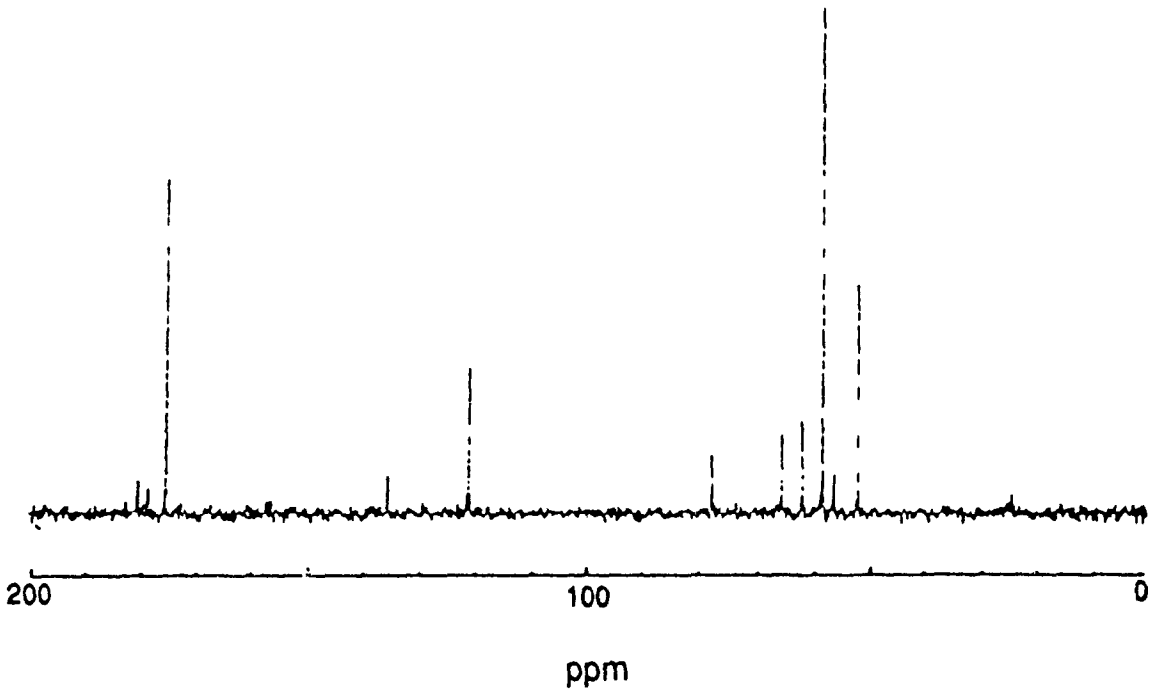

Figure 6.1: Proton Decoupled ^{13}C NMR Spectrum of Enolase Reaction Medium (PGA, EDTA, Mg acetate, Imidazole)

It is the value chosen for θ rather than the delay interval t_D which accomplishes the selectivity of multiplets. with a flip angle of 135°, the CH_2 group will be inverted, the quaternary carbon resonance will be suppressed and the CH group will remain "right side up". Quaternary carbon signals will, of course, be missing from all polarization transfer spectra that are set up to exploit the large single-bond *J*-coupling. In general, DEPT appears to be the preferred polarization transfer method due in large part to its relative insensitivity to the need for a precise matching of the delays and coupling constants.

Fig. 6.2 shows the proton broadband decoupled spectra of PGA in H_2O along with a DEPT sequence applied to it. It is now possible to unambiguously assign the ^{13}C signals as:

COO^-	178.4 ppm
$HCOPO_3$	65.4 ppm
CH_2OH	78.0 ppm

6.2: ^{18}O Exchange

Interconversion of PGA to PEP was carried out in 50% $H_2{}^{18}O$. The initial preliminary experiment was to determine if an upfield shift could be monitored on the carbon directly bound to ^{18}O (in relationship to its detected chemical shift of 78.0ppm). Four time points during the course of the reaction were analyzed, the last being after an overnight incubation allowing for complete equilibrium between PGA and PEP to be established. An upfield shift relative to the resonance position of C_3 carbon attached to ^{16}O was not detected even with expanded scale.

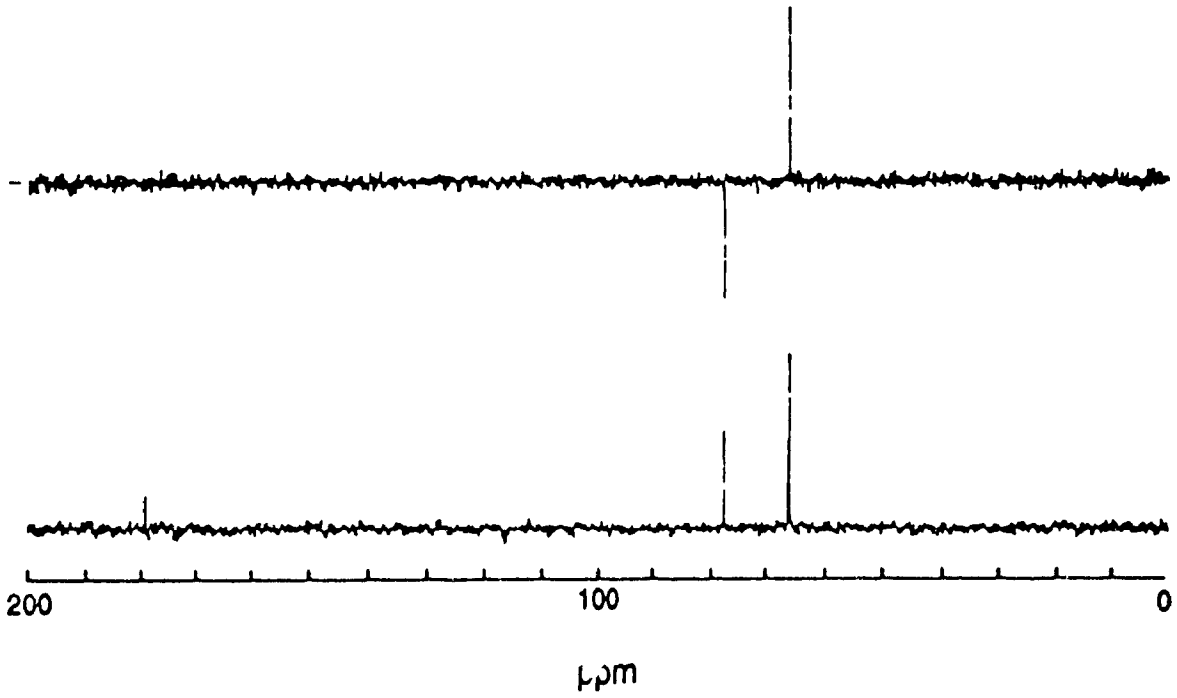

Figure 6.2: Proton Decoupled ^{13}C NMR Spectra of PGA in H_2O with DEPT pulse sequence applied.

The most likely explanation for this disappointing result is that insufficient ^{18}O was incorporated into PGA. In previous studies (Risely and Van Etten, 1979) using tert-butyl alcohol, a distinct peak was seen at 48% incorporation of ^{18}O, a visible shoulder could be detected at 40% and a barely visible shift was seen at 31% ^{18}O. Thus a very high percentage of ^{18}O must be present to see any effect, making the possibility of monitoring relatively early stages in an equilibrium reaction unlikely. Being able to detect additional changes due to the effects of Li^+ seems less likely still.

Another problem inherent with the use of ^{13}C NMR is its relative insensitivity. 25mM PGA is an extremely high substrate concentration to be working with for the determination of kinetic parameters. Yet, it is at the limits of sensitivity for ^{13}C data acquisition. Given that the upfield shift will be on the order of 0.035 - 0.025 ppm (Lombardo et al., 1985) and that we wish to ascertain the effect of Li^+ on this potential upfield shift, the continuance of these experiments seemed suspect. The lack of results, the low probability of future results and the high cost of $H_2{}^{18}O$ led to the conclusion that additional experiments should not be performed.

Conclusions

1) The activity of yeast enolase is inhibited by Li^+, K^+ and Na^+. Less Li^+ than either Na^+ or K^+ is required to produce a given percentage of inhibition. The pattern of inhibition remains the same for all three monovalent cations.

2) At pH 9.2, inhibition by the monovalent cations appears to be competitive with respect to Mg^{2+} (K_m $[Mg^{2+}]$ increasing and V_{max} constant). The apparent change in inhibition patterns from hyperbolic "mixed" at pH 7.1 (Kornblatt and Musil, 1990) to competitive at pH 9.2 may be explained assuming that there has been no change in the enzyme-cation complexes that are formed and that the step inhibited by Li^+ is a fast step in the reaction . Therefore, no decrease in V_{max} is observed. Inhibition at pH 9.2 is thus believed to be partial competitive with respect to Mg^{2+}. A change from partial non-competitive to partially competitive due to a change in the rate limiting step(s) is a more probable explanation than Li^+ now changing its binding site and competing with Mg^{2+} for its binding site.

3) At pH 9.2 the primary kinetic isotope effect on V_{max} decreases to 1.09 ± .12, indicating that there has been a change in the rate limiting step(s) of the reaction with proton abstraction no longer being a slow step. A rate of enzyme catalyzed exchange between the C-2 hydrogen of PGA and solvent of ≃ 50% exchange in remaining PGA after

50% conversion is observed. Li^+ (as well K^+ and Na^+) does not affect the rate of exchange. The results suggest that Li^+ does not inhibit proton abstraction but may inhibit the release of product (either PEP and/or Mg^{2+}).

4) At pH 7.1, there is a kinetic isotope effect on V_{max} of 1.8 for yeast apoenolase activated by Ni^{2+}. With Ni^{2+} activated apoenolase no significant rate of exchange between the C-2 hydrogen of PGA and solvent was measured. From the observed kinetic isotope effect and solvent exchange data we may conclude that for yeast enolase activated by Ni^{2+} at pH 7.1, proton abstraction is still partially rate limiting. In this sense, inhibition by Ni^{2+} may be unique amoung the less effective metals.

5) For apoenolase bound to the non-activator Ca^{2+} no rate of enzyme catalyzed exchange between C-2 hydrogen and solvent could be observed. It is likely that the non-activated enzyme is incapable of proton abstraction.

Further Experiments:

1) More extensive ^{18}O exchange experiments could be performed using higher concentrations of ^{18}O as well as higher field NMR equipment to improve sensitivity. However, it is clearly uncertain whether these improvements alone would allow for detection of the ^{18}O induced ^{13}C upfield shift. The use of ^{13}C enriched PGA would most likely decrease the acquisition time and reduce the amount of material necessary for study of the reaction. Gains in sensitivity by utilization of ^{13}C enriched compounds has been previously shown by Risely and Van Etten(1981).

2) Synthesis of [C_3-^{18}O-PGA]. This potentially may allow for a high enough incorporation of ^{18}O atoms into PGA. If accomplished, the downfield shift due to ^{16}O may be observed.

3) Confirm the step(s) inhibited by Li^+ by performing a stopped-flow experiment at pH 9.2. Stopped flow experiments can detect intermediates that accumulate. At this alkaline pH, proton abstraction is fast compared to the following steps in the reaction , thus the carbanion intermediate should accumulate and a "burst" should be measurable. The first mole of substrate (PGA) rapidly reacts with the enzyme to form stoichiometric amounts of the enzyme-bound intermediate and product, but then the subsequent reaction is slow: there is an initial burst of formation of product (PEP) followed by a progressive increase as the

intermediate turns over. The overall release of product is linear with time after the initial transient and the linear portion extrapolates back to give the magnitude of the burst.

We can now probe for the effects of Li^+. If Li^+ inhibits proton abstraction the magnitude of the burst will decrease (less intermediate may accumulate) whereas if Li^+ inhibits any of the following steps (hydroxyl ion removal or product release or both) the magnitude of the burst will increase.

4) Study the effects of monovalent cations (specifically Li^+) on active monomers of yeast enolase. The monomer of yeast enolase is active provided that high salt has not been used to produce the monomers (Holleman, 1973). Kinetic analysis of activation of the monomers by less effective divalent cations would also be a topic of interest.

5) Study the effects of monovalent cations on active monomers of mammalian enolase. The first demonstration of an active monomer from mammalian (rabbit brain) enolase has been reported by Trepanier et al.(1990). Mammals have three genes which code for enolase; their products are the α, β and γ subunits. Both homo- and hetro-dimers are formed with five of the six possible dimers reported to exist *in vivo* (Rider and Taylor, 1976). Differences exist between these isozymes in terms of sensitivity to salt-induced and pressure-induced inactivation. Trepanier et als. (1990) use of fluorescence polarization for the analysis of inactivation and dissociation showed that the decrease in

activity is a two step process:

Dimer $\rightleftharpoons$ Monomer $\rightleftharpoons$ Monomer*

where monomer* is the inactivated form of the monomer. It would be of great interest to determine whether M is fully active and to perform enzymatic studies on monomer* in order to learn how the detailed mechanism of the inactivated monomer differs from that of the dimmeric enzyme.

6) Perform site directed mutagenesis near the active site or proposed metal-binding sites of yeast enolase and determine the kinetic consequences of these substitutions. The three-dimensional structure of yeast enolase has been determined (Lebioda et al., 1988) to a resolution of 2.25 Å. This structure is based on the amino acid sequence of yeast enolase independently obtained through chemical (Chin et al., 1981) and gene sequencing data (Holland et al., 1981). Having a well defined crystal structure as well as the gene sequence allows for the exploration of structure-function relationships within the enzyme and their effects on various kinetic parameters.

Isolation and confirmation of yeast enolase mutants will not be a trivial task. Yeast contain two nontandemly repeated enolase genes per haploid genome which have been isolated on bacterial plasmids designated peno46 and peno8 (Holland et al, 1981). The corresponding yeast enolase loci have been designated ENO1 and ENO2. Peno46 encodes a polypeptide which closely agrees with the primary structure for the abundant form of enolase isolated from baker's yeast. Immunological and

electrophoretic analyses of the multiple forms of enolase confirms that the two enolase genes are expressed in wild type cells and that isozymes are formed in the cell by random assortment of the two polypeptides into three active enolase dimers (Mcalister and Holland, 1982). To facilitate expression of desired mutants it may be necessary to follow the protocol of Mcalister and Holland where the resident enolase gene in a wild type yeast strain corresponding to the gene isolated on peno46 was replaced with a deletion, constructed *in vitro*, which lacks 90% of the enolase coding sequences. A single form of enolase was resolved from extracts of the deletion mutant cell. Analysis of site-directed mutagenesis at peno8 would thus be greatly simplified.

References

Anderson, V.E., Weiss, P.M., Cleland, W.W., Biochem., 23, 2779-2786 (1984)

Bell, C.F., Principles & Applications of Metal Chelation, Clarendon Press, New York, (1977)

Bovey, F.A., Nuclear Magnetic Resonance Spectroscopy 2nd ed. Academic Press Inc., New York, (1988)

Brewer, J.M., FEBS Letters, 182, # 1, 1-14 (1985)

Brewer, J.M., Crit. Rev. Biochem., 11, 209-254 (1981)

Brewer, J.M. & Collins, K.M., J. Inorg. Biochem., 13, 151-164 (1980)

Brewer, J.M. & Ellis, P.D., J. Inorg. Biochem., 18, 71-82 (1983)

Brewer, J.M. & Weber, G., J. Biol. Chem., 241, # 11, 2550-2557 (1966)

Brewer, J.M., Carriera, L.A., Collins, K.M., Duvall, M.C., Cohen, C., Dervartanian, D.V., J. Inorg. Biochem., 19, 255-267, (1983)

Chin, C., Brewer, J.M, Wold, F., J. Biol. Chem., 256, 1377-1384 (1981)

Cohen, C. & DerVartanian, D.V., J. Inorg. Biochem., 19, 255-267 (1983)

Dinovo, E.C. & Boyer, P.D., J. Biol. Chem., 246, # 11, 4586-4593 (1971)

Duffy, T.H. and Nowak, T., Biochem., 23, 661-670, (1984)

Elliot, J.I. & Brewer, J.M., J. Inorg. Chem., 12, 323-334 (1980)

Fersht, A., Enzyme Structure and Mechanism 2nd ed., W.H. Freeman, New York, (1985)

Hanlon, D.P. and Westhead, E.W, Biochem.,11, 4247-4260 (1969)

Holland, J.M., Holland, J.P., Thill, G.P., Jackson, K.A., J. Biol. Chem., 256, 1385-1395 (1981)

Knack, I. and Rohm, K-H., Hoppe-Seyler's Z. Physiol. Chem, 362, 1119-1130 (1981)

Kornblatt, M.J. & Klugerman, A., Biochem Cell Biol., 67, 103-107 (1989)

Kornblatt, J., Kornblatt, J., Hui Bon Hui, G., Eur. J. Biochem., 128, 577-581 (1982)

Kornblatt, M.J. & Musil, R., Arch. Biochem. Biophys., 277 ,301-305 (1990)

Lebioda, L., Stec, B., Brewer, J.M., J. Biol. Chem., 264, 3685-3693 (1989)

Lebioda, L. and Stec, B., Biochemistry, 30, #11, (1991)

Lebioda, L, Stec, B., Brewer, J.M., Tykaraska, E., Biochemistry, 30, #11, (1991)

Lombardo, D., Fanni, T., Pluckthun, A., Dennis, E.A., J. Bio. Chem, 256, 11663-11666 (1986)

McAlister, Lee and Holland, J.M., J. Biol. Chem., 257, 7181-7188 (1982)

Nowak, T. and Mildvan, A.S., J. Biol. Chem., 245, 6057-6064 (1970)

Nowak, T., Mildvan, A.S. and Kenyon, G.L., Biochemistry, 12, 1690-1701 (1973)

Risely, J.M. & Van Etten, R.L, J. Am. Chem. Soc., 101, 252-253 (1979)

Risley, J.M. & Van Etten, R.L., J. Am. Chem. Soc., 103, 4389-4392 (1981)

Sanders, J.K.M. & Hunter, B.K., Modern NMR Spectroscopy, Oxford University Press, New York, (1987)

Segel, I.H., Enzyme Kinetics, John Wiley and Sons, New York, pp. 161-181 (1975)

Shen, T.Y.S. and Westhead, E.W., Biochemistry, 12, 3333-3337, (1973)

Spring, T.G. and Wold, F., Biochem., 10, 4655-4660, (1971)

Stubbe, J.A. & Abeles, R.H., Biochemistry, 19, 5505-5512 (1980)

Trepanier, D., Wong, C., Kornblatt, M.J., Arch. Biochem Biophys., 283, 271-277 (1990)

Wold, F., Enolase, The Enzymes, Vol. 5, 3rd. ed., Academic Press, New York., pp 499-538 (1971)

Wold, F & Ballou, C.E., J. Biol. Chem., 227, 301-312 (1957)